A&A 615, A175 (2018)
https://doi.org/10.1051/0004-6361/201832711

Astronomy & Astrophysics

Exploring the realm of scaled solar system analogues with HARPS⋆,⋆⋆

D. Barbato[1,2], A. Sozzetti[2], S. Desidera[3], M. Damasso[2], A. S. Bonomo[2], P. Giacobbe[2], L. S. Colombo[4], C. Lazzoni[4,3], R. Claudi[3], R. Gratton[3], G. LoCurto[5], F. Marzari[4], and C. Mordasini[6]

[1] Dipartimento di Fisica, Università degli Studi di Torino, via Pietro Giuria 1, 10125, Torino, Italy
e-mail: barbato@oato.inaf.it
[2] INAF – Osservatorio Astrofisico di Torino, Via Osservatorio 20, 10025, Pino Torinese, Italy
[3] INAF – Osservatorio Astronomico di Padova, Vicolo dell'Osservatorio 5, 35122, Padova, Italy
[4] Dipartimento di Fisica e Astronomia "G. Galilei", Università di Padova, Vicolo dell'Osservatorio 3, 35122, Padova, Italy
[5] European Southern Observatory, Alonso de Córdova 3107, Vitacura, Santiago, Chile
[6] Physikalisches Institut, University of Bern, Sidlerstrasse 5, 3012, Bern, Switzerland

Received 8 February 2018 / Accepted 21 April 2018

ABSTRACT

Context. The assessment of the frequency of planetary systems reproducing the solar system's architecture is still an open problem in exoplanetary science. Detailed study of multiplicity and architecture is generally hampered by limitations in quality, temporal extension and observing strategy, causing difficulties in detecting low-mass inner planets in the presence of outer giant planets.
Aims. We present the results of high-cadence and high-precision HARPS observations on 20 solar-type stars known to host a single long-period giant planet in order to search for additional inner companions and estimate the occurence rate f_p of scaled solar system analogues – in other words, systems featuring lower-mass inner planets in the presence of long-period giant planets.
Methods. We carried out combined fits of our HARPS data with literature radial velocities using differential evolution MCMC to refine the literature orbital solutions and search for additional inner planets. We then derived the survey detection limits to provide preliminary estimates of f_p.
Results. We generally find better constrained orbital parameters for the known planets than those found in the literature; significant updates can be especially appreciated on half of the selected planetary systems. While no additional inner planet is detected, we find evidence for previously unreported long-period massive companions in systems HD 50499 and HD 73267. We finally estimate the frequency of inner low mass (10–30 $M_\oplus$) planets in the presence of outer giant planets as $f_p < 9.84\%$ for $P < 150$ days.
Conclusions. Our preliminary estimate of f_p is significantly lower than the literature values for similarly defined mass and period ranges; the lack of inner candidate planets found in our sample can also be seen as evidence corroborating the inwards-migration formation model for super-Earths and mini-Neptunes. Our results also underline the need for high-cadence and high-precision follow-up observations as the key to precisely determine the occurence of solar system analogues.

Key words. techniques: radial velocities – methods: data analysis – planetary systems – stars: individual: HD 50499 – stars: individual: HD 73267

1. Introduction

The science of exoplanetology has so far produced outstanding results: as of the time of writing (January 2018) the NASA Exoplanet Archive contains data for 3587 confirmed exoplanets, 1509 of which are part of a total of 594 multiple planetary systems. The recent increment in known multiple planets systems, arising in particular from the *Kepler* mission, has helped produce the first comparative studies on their mass distribution and global architecture (see Winn & Fabrycky 2015; Hobson & Gomez 2017). These studies have been especially focused on the multiplicity and architecture's role in supporting or disproving the current and competing formation models for both giant and terrestrial planets as expanded upon in Raymond et al. (2008), Cossou et al. (2014), Schlaufman (2014) and Morbidelli & Raymond (2016).

A key parameter in discriminating between different formation models is the fraction of planetary systems featuring both gas giants and lower-mass planets and their relative orbits; for example the numerical simulations reported in Izidoro et al. (2015) suggest that in situ and inwards-migration formation models of hot super-Earths, defined as planets between 1 and 20 times more massive than the Earth and with orbital periods lower than 100 days, would cause very different systems architecture, the latter creating an anti-correlation between giant planets and close-in super-Earth populations.

However, the investigation of a particular characteristic of multi-planetary systems, namely the frequency of systems featuring a clear mass and dimension hierarchy similar to the one dominating our solar system, suffers from low-quality literature data and would clearly benefit from larger statistics. Out of the 594 multiple planetary systems confirmed so far only two are generally considered to be clear solar system analogues, namely the GJ 676A (Sahlmann et al. 2016) and

⋆ Based on observations collected at the European Organisation for Astronomical Research in the Southern Hemisphere under ESO programmes 093.C-0919(A) and 094.C-0901(A).
⋆⋆ Table 22 is only available at the CDS via anonymous ftp to cdsarc.u-strasbg.fr (130.79.128.5) or via http://cdsarc.u-strasbg.fr/viz-bin/qcat?J/A+A/615/A175

Kepler-90 (Cabrera et al. 2014) systems, and these contain at least one super-Earth, a type of planet noticeably lacking in our own system.

To further support this initial point, lacking a proper review on the subject, we have conducted a preliminary search in the NASA Exoplanet Archive (as retrieved on September 12 2017) in order to provide the required context on the diverse known system architectures, focusing on those systems in which all planetary components have been studied via radial velocity observations. Drawing the line between giant planets and smaller ones at 30 $M_\oplus$, during this search we found that out of the 102 multiple planetary systems studied by RV surveys in which more than half of the planetary components have a catalogued measure of mass, 57 host only giant planets, 24 host only lower-mass planets and only 11 (namely the systems around stars GJ 676 A, GJ 832, HD 10180, HD 11964, HD 164922, HD 181433, HD 190360, HD 204313, HD 219134, HD 219828, and HD 47186) are what could be considered solar system analogues, featuring inner low-mass planets and outer giant planets orbiting outside the circumstellar habitable zone outer limit, computed here using the model discussed in Kopparapu et al. (2013). Finally we note the existence of ten mixed-architecture multiple systems, featuring giant planets on close-in orbits or inside the habitable zone. We can therefore provide a preliminary estimate of known solar system analogues amounting to about 10% of known multiple systems studied by RV surveys.

This fraction is highly dependent on the exact definition of what constitutes a solar system analogue. For example, it is significantly larger if one considers only the giant planets orbital periods instead of their position relative to the system's habitable zone as key to architectural characterization; considering as analogues those systems composed of inner lower-mass planets and outer giants whose orbits are longer than 1 yr this fraction amounts to 15.57% of known multiple systems, and to 19.67% if the lower limit on giant planets orbital period is instead set at 100 days.

Although small, this fraction is an encouraging sign that a sizeable number of planetary systems may reproduce our own planetary architecture, featuring at least one gas giant on a long-period orbit and lower-mass planets on inner orbits. Another positive clue can be identified in the findings of Ciardi et al. (2013), suggesting that in up to 60% of *Kepler* candidate planet pairs the innermost one has a smaller radius than the outer body, and that this fraction rises up to 68% if the pair contains one Neptune-sized planet. Winn & Fabrycky (2015) also reports that approximately half of Sun-like star host at least one small planet (from 1 to 4 $R_\oplus$) with an orbital period of less than 1 yr.

During the aforementioned preliminary search through the RV-observed known systems we found 229 single-planet systems, 195 of which contain a single long-period ($P \geq 1$ yr) giant and 34 containing a single Neptune-like or super-terrestrial planet. In this context, it is clear that this large known fraction of long single-period giant planet systems may represent an unparalleled opportunity for the search of yet undetected inner, smaller planets and therefore of scaled-down solar system analogues. However, known systems with giant planets are not usually subject to follow-up observations searching for additional, lower mass planetary companions at short orbital period. Furthermore, the available data published on most of these systems alone does not provide enough solid ground on which to base such a search, as it is characterized by a sampling frequency and in some cases an integration time or instrument setup unsuited to detecting low-mass and short period planets. To successfully detect such inner planets and their very low amplitude signals compared to those of the more massive and distant companions, intense monitoring of the host star is needed in order to fully cover their orbital phase. The need for higher precision and more densely sampled observations on already studied planetary systems is therefore clear and urgent in the search for scaled-down solar system analogues.

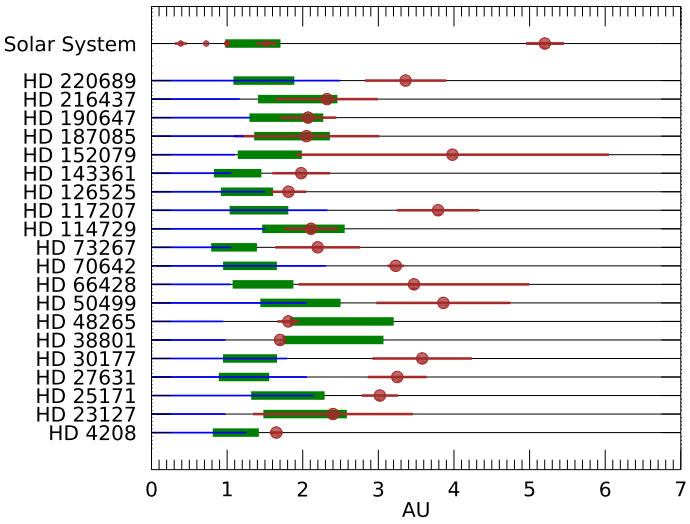

Fig. 1. Overview of the sample systems and a comparison with the inner solar system architecture. Known giant planets of the sample are shown as brown circles, a thin brown line from periastron to apoastron showing their orbit's span. Each system's habitable zone, computed using the model detailed in Kopparapu et al. (2013), is shown as a thick green band, while the thin blue line indicates each system's region of dynamical stability for additional inner planets as computed through Hill's criterion detailed in Sect. 4.

The purpose of this paper is therefore to present the results of the observations conducted by the HARPS spectrograph on a small sample of these single-giant systems, in order to provide an estimate of the occurence rate of smaller inner planets in the presence of a single outer giant planet and to fuel further observations. We also note that the analysis of a parallel HARPS-N survey on a similarly selected northern hemisphere sample is currently underway and will be the subject of a forthcoming paper.

In Sect. 2 we describe the selection criteria for the analyzed sample, before moving on to describe the HARPS observations structure and setup in Sect. 3. In Sect. 4 we show the results of the new data fits conducted to refine the orbital parameters of the known planets. Finally, in Sect. 5 we calculate the detection limits for each system and the sample as a whole, in order to provide an estimate to the planetary frequency of low-mass inner planets in the presence of outer giant planets to compare with the planetary frequency calculated in the seminal work of Mayor et al. (2011) for stars hosting at least one planet.

2. Sample selection and description

The 20 southern-emisphere stars selected for this work are all bright ($V < 9.2$), inactive ($\log R'_{\rm HK} < -4.8$), not significantly evolved ($\log g > 4$) and are not members of visually close binaries. This set of criteria ensures that the overall sample is well suited to the search for low-mass inner planets.

All systems feature a single giant planet orbiting the host star at low to moderate eccentricities ($e < 0.5$), with periastron larger than 1 AU and discovered via the radial velocity method. Additional details of each system's stellar parameters

Table 1. Stellar parameters for the sample systems.

Star	π (mas)	V (mag)	B-V[a] (mag)	$T_{\rm eff}$ (K)	log$g$[a] (cgs)	[Fe/H]	Mass[a] ($M_\odot$)	Radius[a] ($R_\odot$)	Age[a] (Gyr)	log $R'_{\rm HK}$	$P^{e}_{\rm rot}$ (d)
HD 4208	30.58 ± 1.08	7.795 ± 0.011	0.726 ± 0.008	5717 ± 33[b]	4.501 ± 0.036	−0.28 ± 0.02	0.883 ± 0.024	0.846 ± 0.028	3.813 ± 2.970	−4.77	∼25
HD 23127	11.22 ± 0.76	8.576 ± 0.002	0.701 ± 0.013	5843 ± 52[b]	4.146 ± 0.054	0.29 ± 0.03	1.208 ± 0.045	1.490 ± 0.104	4.508 ± 0.788	−5.00	∼33
HD 25171	17.84 ± 0.60	7.782 ± 0.013	0.618 ± 0.005	6125 ± 21[b]	4.263 ± 0.031	−0.12 ± 0.04	1.076 ± 0.021	1.230 ± 0.045	4.802 ± 0.619	−4.99	∼22
HD 27631	22.45 ± 0.78	8.243 ± 0.012	0.721 ± 0.009	5737 ± 36	4.455 ± 0.038	−0.12 ± 0.05	0.944 ± 0.032	0.923 ± 0.033	4.010 ± 2.892	−4.91	∼31
HD 30177	19.93 ± 0.63	8.397	0.773 ± 0.012	5607 ± 47[b]	4.417 ± 0.034	0.39 ± 0.05	1.053 ± 0.023	1.019 ± 0.034	2.525 ± 1.954	−5.07	∼45
HD 38801	10.39 ± 1.74	8.224	0.841 ± 0.019	5338 ± 59[b]	3.877 ± 0.084	0.25 ± 0.03	1.207 ± 0.108	2.029 ± 0.286	6.072 ± 1.835	−5.03	∼47
HD 48265	11.48 ± 0.72	8.051	0.722 ± 0.013	5733 ± 55[d]	3.970 ± 0.048	0.30 ± 0.04	1.312 ± 0.064	1.901 ± 0.126	4.201 ± 0.625	−5.21	∼45
HD 50499	21.02 ± 0.68	7.207 ± 0.004	0.628 ± 0.014	6102 ± 54[b]	4.247 ± 0.033	0.26 ± 0.04	1.253 ± 0.020	1.351 ± 0.054	2.391 ± 0.633	−5.03	∼25
HD 66428	18.21 ± 1.07	8.246 ± 0.013	0.717 ± 0.006	5773 ± 23[b]	4.360 ± 0.050	0.23 ± 0.05	1.083 ± 0.022	1.102 ± 0.062	3.515 ± 2.040	−5.07	∼38
HD 70642	34.84 ± 0.60	7.169	0.733 ± 0.005	5732 ± 23[b]	4.458 ± 0.017	0.22 ± 0.02	1.078 ± 0.015	0.984 ± 0.022	0.919 ± 0.733	−4.90	∼32
HD 73267	18.77 ± 1.00	8.889	0.827 ± 0.003	5387 ± 10[d]	4.447 ± 0.035	0.07 ± 0.04	0.897 ± 0.019	0.909 ± 0.033	8.140 ± 3.505	−4.97	∼43
HD 114729	27.69 ± 0.54	6.687 ± 0.005	0.688 ± 0.003	5844 ± 12[c]	4.046 ± 0.016	−0.33 ± 0.03	0.936 ± 0.013	1.473 ± 0.037	10.116 ± 0.344	−5.07	∼34
HD 117207	30.37 ± 0.92	7.240	0.727 ± 0.014	5732 ± 53[b]	4.371 ± 0.039	0.19 ± 0.03	1.053 ± 0.028	1.074 ± 0.041	4.192 ± 2.274	−5.06	∼39
HD 126525	26.24 ± 0.82	7.847 ± 0.004	0.747 ± 0.003	5638 ± 13[c]	4.382 ± 0.028	−0.10 ± 0.01	0.897 ± 0.010	0.979 ± 0.030	9.670 ± 1.333	−5.03	∼40
HD 143361	16.80 ± 1.26	9.200	0.792 ± 0.004	5507 ± 10[d]	4.472 ± 0.043	0.14 ± 0.06	0.968 ± 0.027	0.916 ± 0.041	2.942 ± 2.749	−5.00	∼42
HD 152079	11.90 ± 1.40	9.182	0.687 ± 0.014	5907 ± 52	4.365 ± 0.054	0.29 ± 0.07	1.147 ± 0.030	1.128 ± 0.074	1.622 ± 1.369	−4.99	∼31
HD 187085	22.02 ± 1.12	7.225	0.622 ± 0.007	6117 ± 27[b]	4.279 ± 0.041	0.12 ± 0.04	1.189 ± 0.023	1.270 ± 0.066	2.747 ± 0.838	−4.93	∼21
HD 190647	18.70 ± 1.10	7.779	0.744 ± 0.017	5656 ± 60[b]	4.162 ± 0.054	0.23 ± 0.02	1.069 ± 0.027	1.376 ± 0.089	7.957 ± 1.096	−5.09	∼42
HD 216437	37.58 ± 0.56	6.057 ± 0.001	0.677 ± 0.009	5909 ± 31[b]	4.188 ± 0.026	0.20 ± 0.10	1.165 ± 0.046	1.394 ± 0.032	4.750 ± 1.059	−5.01	∼30
HD 220689	21.96 ± 0.92	7.795 ± 0.062	0.671 ± 0.007	5921 ± 26	4.360 ± 0.045	−0.07 ± 0.10	1.016 ± 0.048	1.068 ± 0.047	4.586 ± 2.487	−4.99	∼29

Notes. All stellar data retrieved from Vizier catalogue, except: [(a)]Calculated from PARAM 1.3 (see da Silva et al. 2006). [(b)]Retrieved from Bonfanti et al. (2015). [(c)]Retrieved from Sousa et al. (2008). [(d)]Retrieved from Stassun et al. (2017). [(e)]Calculated following Mamajek & Hillenbrand (2008).

can be found in Table 1, while a global overview of the planet positions relative to stars and habitable zones is given in Fig. 1; all planetary data were retrieved from the most recent published paper discussing each planet's orbital solution and listed in the first column of Tables 2–21. Regarding stellar parameters, each star's parallax, visual magnitude, metallicity, and $\log R'_{\rm HK}$ were retrieved from the Vizier online catalogue; effective temperatures were instead retrieved by joining the estimates reported in Bonfanti et al. (2015), Sousa et al. (2008) and Stassun et al. (2017). These stellar parameters were then used as inputs into the online tool PARAM to calculate each star's colour index, surface gravity, mass, radius, and age as detailed in da Silva et al. (2006). Values of stellar rotational period were instead computed using the empirical relations between $(B-V)$, $\log R'_{\rm HK}$ and $P_{\rm rot}$ from Noyes et al. (1984) and Mamajek & Hillenbrand (2008) and here reported with a one-day precision for the analytical nature of the relations used.

At a general overview of the system characteristics, it can be noted that all selected stars are reasonably similar to our Sun. The two stars HD 38801 and HD 48265 are noteworthy exceptions, whose mass and size (respectively 1.36 $M_\odot$, 2.53 $R_\odot$ and 1.28 $M_\odot$, 2.05 $R_\odot$) suggest that they are in a later stage of their evolution, probably on the sub-giant branch.

Moving on to the planets in the chosen sample, the minimum mass range spans from 0.224 $M_{\rm J}$ to 10.7 $M_{\rm J}$, the most massive planet being HD 38801 b, which also features peculiar zero values of eccentricity and periastron longitude as fixed in the discovery paper (Harakawa et al. 2010) to improve its Keplerian fit quality. Such a low value of eccentricity at such intermediate distances from the host star (a = 1.7 AU), it is noted, cannot yet be explained by tidal circularization and therefore represents an interesting conundrum. All the planets in the sample are characterized by long-period orbits, spanning from 1.89 to 7.94 yr, and low to moderate eccentricities ($e < 0.52$).

It is also important to note that although each selected system was known to host a single, giant planet at the beginning of our observational programme, an additional outer giant planet has been recently discovered in the system HD 30177, as detailed in Wittenmyer et al. (2017). Still, we have nonetheless decided to show rather than discard the results of our observations and analysis on this system, both since the existence of HD 30177 c was not known at the time of observation and because its very long period (P = 31.82 yr) causes it not to have a significant dynamical influence on the short-period regions of interest to our study. We further stress the fact that through extensive simulations using literature and archival RV data, we verified that current data on the selected sample do not provide the sensitivity needed to succesfully detect Neptune-mass planets with $P < 50d$, due to large RV errors ($\geq$5 m s^{-1}) in the discovery data, poor sampling at short periods, or both.

3. HARPS observations

As discussed in Sect. 1, the present understanding of multiple planetary systems architecture still shows severe gaps, especially regarding the occurence of architectures mimicking that of our solar system. To try to help filling these gaps we have conducted intense monitoring on selected stars hosting a single long-period giant planet using the high-precision HARPS spectrograph mounted at the ESO La Silla 3.6 m telescope. In order to successfully detect any additional low-mass planets in the selected systems and to further refine the outer giant planet orbit, the selected stars were intensely observed over a time period spanning from April 2014–March 2015 (ESO programmes 093.C-0919(A) and 094.C-0901(A)). During this period each star was observed for about a semester, and to optimize time sampling the observing nights were split into blocks of two or three nights at the beginning, middle and end of the observing period. Based on the allocated observation time a total of 514 measurements where obtained during this period, providing about 27 datapoints on average for each of the 20 target stars. This number of observations, we note, is significantly lower than the ~40 measurements per star that we originally foresaw in the programme proposal.

Depending on magnitude, the target stars were measured with 10 or 15 min total exposure, in order to achieve sufficient signal-to-noise ratio (S/N) to reach the required <1 m s^{-1} precision for all programme stars using HARPS in its simultaneous Th-Ar observing mode. The aforementioned integration time was also needed to average the oscillation and granulation modes of solar-type stars.

4. Systems analysis

4.1. Fitting methodology

A complete list of the newly acquired high-precision HARPS data for each system in the selected sample is collected in Table 22. To use this data for the refinement of the known planets orbital elements we subtracted from the raw timeseries the stellar proper radial motion computed as the mean of the radial velocity dataset. We then added all the literature data available on each system to our datasets, producing therefore a complete series of radial velocity data comprising discovery datasets, follow-up timeseries, and the HARPS data acquired during our survey; when available previous HARPS observations publicly released on the ESO archive were also used. Any HARPS datapoint characterized by a S/N lower than 30 was removed; details on the excluded datapoints are to be found in the paragraphs for each system in Sect. 4.3. Unless otherwise noted, we fitted for no offset between the various HARPS datasets, that were therefore treated as a single timeseries. The main purpose of joining various datasets from different observations and instruments is to use the higher precision of HARPS data to further constrain and refine the known planets orbital parameters by refitting the complete timeseries composed of both historic and new data.

The fits have been obtained using the `EXOFAST` suite of routines written for IDL (Eastman et al. 2013), characterizing the orbital parameters and their uncertainties with a differential evolution Markhov chain Monte Carlo method, the fitting parameters being time of periastron $T_{\rm peri}$, orbital period P, $\sqrt{e}\cos\omega$, $\sqrt{e}\sin\omega$, semi-amplitude K and systematic velocity $\gamma_{\rm i}$ and jitter $j_{\rm i}$ for each instrument in the joined timeseries. The `EXOFAST` routines assumes the stellar jitter to be uncorrelated Gaussian noise that is added in quadrature to the radial velocity measurement error. The known orbital parameters found in the literature and listed in Tables 2–21 were used as starting estimates for the MCMC chains to help achieve a better convergence.

After subtracting the best-fit Keplerian curve produced by `EXOFAST`, the residual datapoints were used to produce a generalized Lomb-Scargle periodogram using the IDL routine `GLS` (Zechmeister & Kürster 2009). This allowed us to investigate the presence of additional inner planetary signals, selecting as signals of potential interest for further investigation only those power peaks characterized by a false alarm probabilty as computed via bootstrap method less than or equal to 1%.

As a further note on the plausibility of the presence of additional inner planets, after obtaining the refined fits on each

system we searched for the maximum orbital period allowing dynamical stability for a single additional planet on a circular inner orbit under the gravitational influence of the known outer planet, using the equality on Hill's criterion (see e.g. Murray & Dermott 1999):

$$a_1(1-e_1) - a_2 \geq 2\sqrt{3}R_H \quad (1)$$

being a_1 and e_1 the major semiaxis and eccentricity of the known giant planet, a_2 the major semiaxis of the test planet's orbit and R_H the known planet's Hill radius defined as:

$$R_H = a_1(1-e_1)\sqrt[3]{\frac{m_1}{3M_*}}. \quad (2)$$

We therefore considered the maximum approach distance between the known outer giant planet and the inner test planet as the limit stability. We varied the test planet's mass in the range 0.1–2 M_J and, since the maximum stable period for the test planet underwent a variation amount to less than one day within this mass range, we provide a mean value for this maximum stable period in the paragraph for each system in Sect. 4.3, and show each system's stability region as a thin blue line in Fig. 1. Details on overall results and on case-by-case fitting process and results are to be found below.

4.2. Overview of results

The overall results of the new fits obtained joining our HARPS high-precision data with the available literature time series can be roughly divided in three main categories: fits that confirm the literature without significant changes to the orbital solution; fits that instead significantly change some or all of the published orbital elements; and fits that suggest the existence of additional planetary companions in the system. A comparison between the literature results and the parameters obtained from our MCMC chains is shown for each system in Tables 2–21, along with the number of measurements used for each orbital solution and the mean radial velocity error for each dataset. It is interesting to note that the values for stellar jitter derived from our orbital solutions are often different between the used dataset, the lowest being usually the one found for HARPS datasets; this may suggest that the jitter is likely dominated by instrumental effects for instruments with lower precision than HARPS.

Out of the 20 planetary systems of our sample, seven did not significantly benefit from the addition of our new, higher-precision HARPS data, resulting in new orbital solution compatible with the ones found in the literature (HD 23127, HD 25171, HD 27631, HD 114729, HD 117207, HD 187085, and HD 220689). We do, however, note that for the most part our orbital solutions feature higher-precision orbital parameters.

Instead, the addition of the HARPS data obtained from our observations brought significant updates in 12 systems of the sample (HD 4208, HD 30177, HD 38801, HD 48265, HD 66428, HD 70642, HD 73267, HD 126525, HD 143361, HD 152079, HD 190647, and HD 216437). For the most part these updates consist of eccentricity values and periods that are incompatible with those found in the literature best-fits solutions. We also want to explicitly stress that our data produced very different orbital parameters for planet HD 30177 c, the addition of orbital parameters missing in the literature fit for HD 126525 and the detection of a linear trend not previously published for HD 73267. Finally, we report the characterization of outer giant planet HD 50499 c, the existence of which could be previously inferred in the quadratic trend of Keck data but was never fitted and published before.

Table 2. Fit results comparison for system HD 4208.

	HD 4208	
	Butler et al. (2006)	This work
Parameter	Planet b	Planet b
K (m s^{-1})	19.06 ± 0.73	$19.03^{+0.85}_{-0.79}$
P (days)	828.0 ± 8.1	$832.97^{+2.15}_{-1.89}$
$\sqrt{e}\cos\omega$	–	$-0.101^{+0.148}_{-0.121}$
$\sqrt{e}\sin\omega$	–	$-0.092^{+0.147}_{-0.123}$
e	0.052 ± 0.040	$0.042^{+0.039}_{-0.029}$
ω (deg)	345	$217.634^{+57.556}_{-67.497}$
$M\sin i$ (M_J)	0.804 ± 0.073	$0.810^{+0.014}_{-0.015}$
a (AU)	1.650 ± 0.096	$1.662^{+0.015}_{-0.015}$
T_{peri} (d)	2451040 ± 120	$2456505.5^{+127.3}_{-491.3}$
n_{obs}	52	82

	Mean RV error (m s^{-1})	γ (m s^{-1})	Jitter (m s^{-1})
Keck1	1.52	$0.12^{+0.58}_{-0.58}$	$3.26^{+0.55}_{-0.45}$
Keck2	1.44	$-12.39^{+1.99}_{-1.99}$	$6.36^{+1.86}_{-1.30}$
HARPS	0.48	$-17.31^{+0.88}_{-0.86}$	$1.33^{+0.23}_{-0.19}$

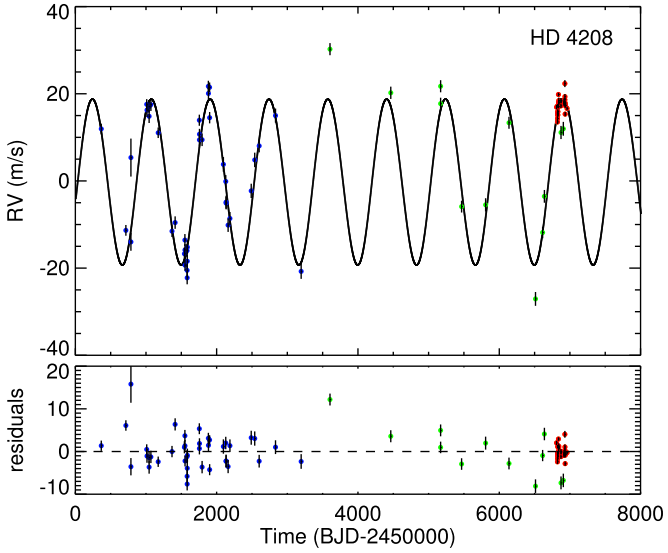

Fig. 2. Analysis results for system HD 4208. In the *top panel*, our best-fit solution is superimposed as a black curve on the literature datapoints from two Keck surveys (shown in blue and green) and from our HARPS observations (shown in red). *Bottom panel*: residual radial velocities obtained after subtracting our best-fit solution for HD 4208 b from the original datapoints.

4.3. Case-by-case results

HD 4208. The only planetary companion of this G5V star was first detected by Vogt et al. (2002) via 35 Keck observations spanning about 5 yr. Later observations and improvements in data reduction pipelines reported in Butler et al. (2006) have refined the planet's orbital parameters; additional and further refined Keck data have recently been published in Butler et al. (2017), although no further orbital refinement has yet been anounced.

Table 3. Fit results comparison for system HD 23127.

HD 23127		
Parameter	O'Toole et al. (2007) Planet b	This work Planet b
K (m s^{-1})	27.5 ± 1	$27.72^{+2.83}_{-2.63}$
P (days)	1214 ± 9	$1211.17^{+11.11}_{-8.91}$
$\sqrt{e}\cos\omega$	–	$-0.613^{+0.088}_{-0.065}$
$\sqrt{e}\sin\omega$	–	$-0.019^{+0.176}_{-0.185}$
e	0.44 ± 0.07	$0.406^{+0.083}_{-0.09}$
ω (deg)	190 ± 6	$181.829^{+17.296}_{-16.507}$
$M \sin i$ (M_J)	1.5 ± 0.2	$1.527^{+0.037}_{-0.038}$
a (AU)	2.4 ± 0.3	$2.370^{+0.032}_{-0.032}$
T_{peri} (days)	2450229 ± 19	$2457266.6^{+62.1}_{-43.5}$
n_{obs}	34	58
	Mean RV error (m s^{-1})	γ (m s^{-1})	Jitter (m s^{-1})
AAT	4.30	$5.55^{+2.32}_{-2.27}$	$11.00^{+2.01}_{-1.60}$
HARPS	0.64	$-1.82^{+4.69}_{-4.53}$	$1.88^{+0.38}_{-0.29}$

Table 4. Fit results comparison for system HD 25171.

HD 25171		
Parameter	Moutou et al. (2011) Planet b	This work Planet b
K (m s^{-1})	15.0 ± 3.6	$14.56^{+0.84}_{-0.88}$
P (days)	1845 ± 167	$1802.29^{+24.12}_{-22.92}$
$\sqrt{e}\cos\omega$	–	$-0.006^{+0.175}_{-0.169}$
$\sqrt{e}\sin\omega$	–	$0.028^{+0.159}_{-0.169}$
e	0.08 ± 0.06	$0.042^{+0.046}_{-0.029}$
ω (deg)	96 ± 89	$159.543^{+136.626}_{-104.900}$
$M \sin i$ (M_J)	0.95 ± 0.10	$0.915^{+0.011}_{-0.012}$
a (AU)	3.02 ± 0.16	$2.971^{+0.033}_{-0.032}$
T_{peri} (days)	2455301 ± 449	$2457105.7^{+540.5}_{-554.43}$
n_{obs}	24	46
	Mean RV error (m s^{-1})	γ (m s^{-1})	Jitter (m s^{-1})
HARPS	1.18	$-2.10^{+0.60}_{-0.58}$	$2.40^{+0.39}_{-0.34}$

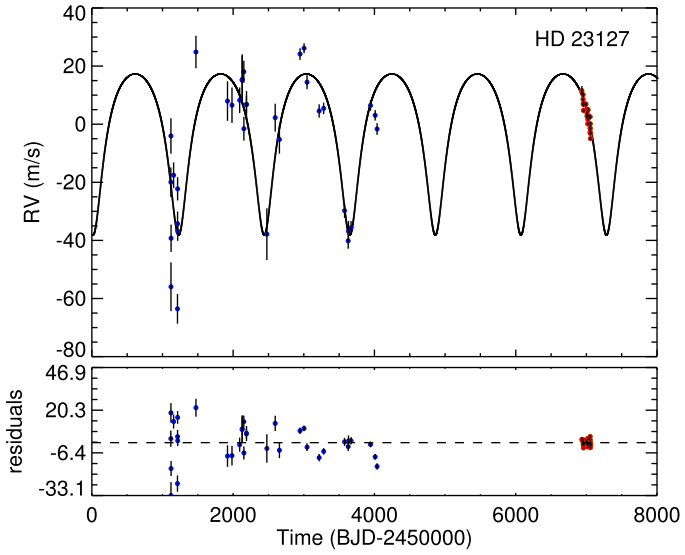

Fig. 3. Same as Fig. 2 but for system HD 23127. The literature AAT data are shown in blue, while our HARPS survey data are shown in red.

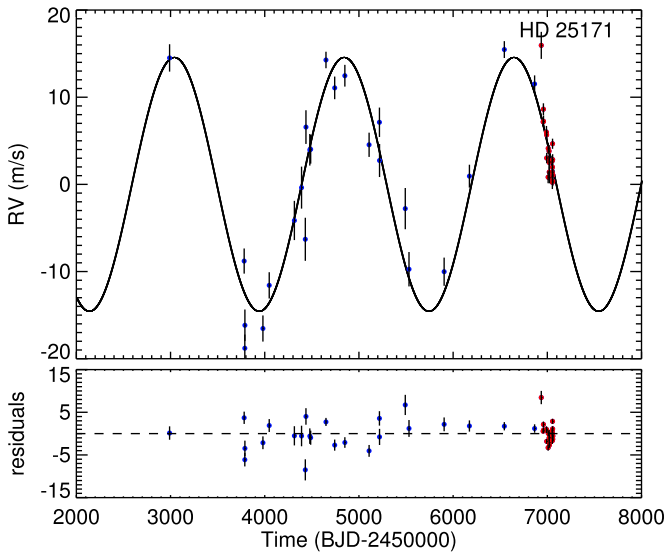

Fig. 4. Same as Fig. 2 but for system HD 25171. The literature HARPS data are shown in blue, while our HARPS survey data are shown in red.

Using all these literature results as historical data next to the 30 high-precision datapoints obtained during our HARPS survey we obtained a new orbital fit (see Table 2 and Fig. 2) with Keplerian semi-amplitude $K = 19.03^{+0.85}_{-0.79}$ m s^{-1} and period $P = 832.97^{+2.15}_{-1.89}$ d, from which we estimated the minimum mass of HD 4208 b to be $M \sin i = 0.810^{+0.014}_{-0.015}\,M_J$, its eccentricity as $e = 0.042^{+0.039}_{-0.029}$ and a longitude of periastron of $\omega = 217.634^{+57.556°}_{-67.497}$.

Our results are generally compatible with Butler's, although better constrained; an exception is represented by a very different value of ω. No power peak with FAP ≤ 0.01 was found in the residual data periodogram. Using the Hill criterion we also find the maximum dynamically stable period for an inner planet to be 547.5 days.

HD 23127. A G2V star, HD 23127's planetary companion was announced in O'Toole et al. (2007) based on 34 observations collected at the Anglo-Australian Telescope (AAT) over 7.7 yr; no further data nor refinement to the planet's orbital elements have been published since its discovery.

The HARPS observations have produced 25 new datapoints; we excluded a single datapoint taken at epoch 2456989.5 since it showed a radial velocity difference from the observation taken the previous and following nights of ~30 m s^{-1}, in addition to having an outlier value of bisector. As it is so different, this is difficult to justify as a real radial velocity variation and the point was flagged as spurious, probably due to some error

Table 5. Fit results comparison for system HD 27631.

HD 27631		
Parameter	Marmier et al. (2013) Planet b	This work Planet b
K (m s^{-1})	23.7 ± 1.9	$24.51^{+1.84}_{-1.82}$
P (days)	2208 ± 66	$2198.14^{+54.11}_{-50.34}$
$\sqrt{e}\cos\omega$	–	$-0.182^{+0.177}_{-0.143}$
$\sqrt{e}\sin\omega$	–	$0.284^{+0.113}_{-0.159}$
e	0.12 ± 0.060	$0.141^{+0.062}_{-0.065}$
ω (deg)	134 ± 44	$122.642^{+33.335}_{-30.158}$
$M \sin i$ (M_J)	1.45 ± 0.14	$1.494^{+0.042}_{-0.042}$
a (AU)	3.25 ± 0.07	$3.242^{+0.070}_{-0.068}$
T_{peri} (days)	2453867 ± 224	$2456086.0^{+193.4}_{-170.8}$
n_{obs}	64	87

	Mean RV error (m s^{-1})	γ (m s^{-1})	Jitter (m s^{-1})
CORALIE1	5.84	$8.19^{+3.24}_{-3.28}$	$5.29^{+1.97}_{-1.74}$
CORALIE2	3.76	$-3.74^{+1.59}_{-1.68}$	$7.42^{+1.19}_{-1.05}$
HARPS	0.53	$-1.79^{+3.31}_{-3.47}$	$4.24^{+0.79}_{-0.61}$

occurring during its acquisition, and therefore ignored in the subsequent analysis.

The orbital fit (see Table 3 and Fig. 3) obtained from joining the 34 AAT datapoints with the 24 HARPS observations suggests new orbital elements values of $M \sin i = 1.527^{+0.037}_{-0.038}\ M_J$, $P = 1211.17^{+11.11}_{-8.91}$ d and $e = 0.406^{+0.083}_{-0.09}$, results compatible with the literature solution. The radial velocity residuals periodogram show no power peak under the 0.01 level of FAP, and we find the maximum stable period for an additional inner planet to be 322.1 days.

HD 25171. The planet of this F8V-type star was discovered and characterized in Moutou et al. (2011) via 24 HARPS observations; eight additional HARPS datapoints are publicly accessible from the ESO Science Archive. Of these 32 archival HARPS data we excluded a total of eight datapoints due to a S/N lower than 30, namely the data found at epochs 2452946.79, 2452998.59, 2454732.77, 2454813.77, 2455091.89, 2455105.77, 2455261.53, and 2456751.48.

In addition to this literature HARPS data we used our own 22 lower-uncertainties datapoints to obtain a $K = 14.56^{+0.85}_{-0.88}$, $P = 1802.29^{+24.12}_{-22.92}$ d Keplerian fit (see Table 4 and Fig. 4) from which we provide new estimates of minimum mass of $0.915^{+0.012}_{-0.012}\ M_J$ and eccentricity of $0.0417^{+0.046}_{-0.029}$, in a generally good agreement with the literature fit. No power peak with a sufficiently low false alarm probability is present in the residuals periodogram. The maximum stable period for an inner planet found via the Hill criterion is 1105 days.

HD 27631. The planet orbiting this G3IV star was first discovered by Marmier et al. (2013) using a total of 64 CORALIE measurements. The final 37 of these measurements were obtained after an upgrade of the instrument and are therefore treated as a separate dataset with its own radial velocity offset.

During our HARPS observations we have obtained 23 further datapoints; the joined time series was then used to produce

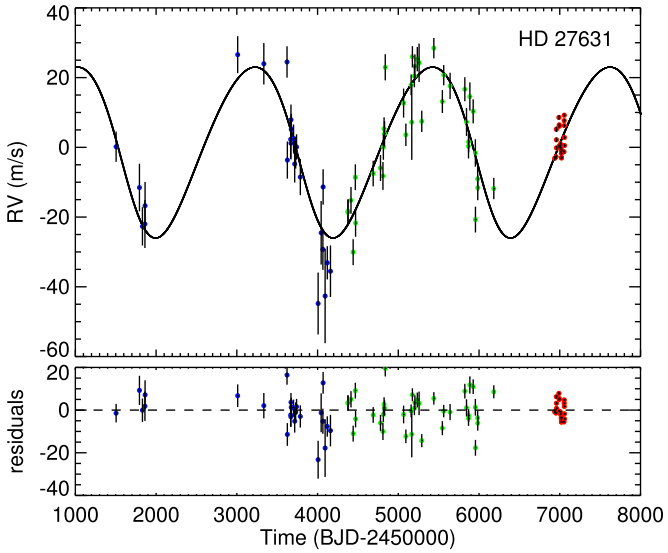

Fig. 5. Same as Fig. 2 but for system HD 27631. The literature CORALIE surveys data are shown in blue and green, while our HARPS survey data are shown in red.

a Keplerian fit having semi-amplitude $K = 24.51^{+1.84}_{-1.82}$ m s^{-1} and period $P = 2198.14^{+54.11}_{-50.34}$ d, providing a new estimate of $M \sim i = 1.494^{+0.042}_{-0.042}\ M_J$ and eccentricity $e = 0.141^{+0.062}_{-0.065}$, an overall solution compatible yet better constrained than the literature fit (see Table 5 and Fig. 5). We also find the maximum stable period for an additional inner planet to be 1107 days. Finally, the generalized Lomb-Scargle periodogram produced from the residual data features no major peak with FAP ≤ 0.01.

HD 30177. The planetary system orbiting this G8V star is a well-studied one and therefore deserves special attention. The first study to detect a planet around the star (Tinney et al. 2003) used fifteen AAT observations and failed to observe the planet's entire orbit, leading to noticeably poor constrained values of $e = 0.22 \pm 0.17$ and $M \sin i = 7.7 \pm 1.5\ M_J$. A follow-up study (Butler et al. 2006) refines these values leading to estimates of $e = 0.193 \pm 0.025$ and a minimum mass of $10.45 \pm 0.88\ M_J$. Most recently, Wittenmyer et al. (2017) reports an orbital fit made from 28 additional AAT data and 20 HARPS-TERRA measurements, leading to the latest values of $M \sin i = 8.08 \pm 0.10\ M_J$, $P = 2524.4 \pm 9.8$ d, $e = 0.184 \pm 0.012$; of particular interest is the fact that the authors best-fit solution feature an additional, outer planetary companion HD 30177 c, estimating a minimum mass of $7.60 \pm 3.10\ M_J$, a period of 11613 ± 1837 days and an eccentricity value of 0.22 ± 0.14.

As already noted and discussed in Sect. 2, the existence of planet c was not known during our targets selection and subsequent HARPS observations, hence the inclusion of this system in an otherwise single-planet sample. We decided nevertheless to include HD 30177 in this paper, since we consider the published outer companion's long period of 31.82 yr not to have a significant dynamical influence in the stability of the short-period ($a < 1$ AU) region of interest in searching for inner, low-mass companions. We therefore report here the result of the fit obtained joining the literature data to the additional 26 HARPS measurements collected in our observations, noting that we excluded from the following analysis four datapoints taken at epochs 2454384.87, 2455563.54, 2455564.57 and 2456631.80 due to low S/N.

It can be noted that the dataset used in Wittenmyer et al. (2017) fails to cover a significant portion of the orbit of

Table 6. Fit results comparison for system HD 30177.

HD 30177				
Parameter	Wittenmyer et al. (2017) Planet b	This work Planet b	Wittenmyer et al. (2017) Planet c	This work Planet c
K (m s^{-1})	126.3 ± 1.5	$125.98^{+1.26}_{-1.27}$	70.8 ± 29.5	≥16.42
P (days)	2524.4 ± 9.8	$2527.83^{+4.71}_{-4.69}$	11613 ± 1837	≥6163.40
$\sqrt{e}\cos\omega$	–	$0.340^{+0.014}_{-0.014}$	–	–
$\sqrt{e}\sin\omega$	–	$0.216^{+0.015}_{-0.016}$	–	–
e	0.184 ± 0.012	$0.162^{+0.010}_{-0.010}$	0.22 ± 0.14	–
ω (deg)	31 ± 3	$32.422^{+2.525}_{-2.563}$	19 ± 30	–
$M \sin i$ (M_J)	8.08 ± 0.10	$8.622^{+0.125}_{-0.126}$	7.6 ± 3.1	≥1.533
a (AU)	3.58 ± 0.01	$3.704^{+0.027}_{-0.027}$	9.89 ± 1.04	–
T_{peri} (days)	2451434 ± 29	$2456502.4^{+17.9}_{-18.4}$	2448973 ± 1211	–
n_{obs}	63	85		
	Mean RV error (m s^{-1})	γ (m s^{-1})	Jitter (m s^{-1})	
AAT	3.84	$22.16^{+1.69}_{-1.73}$	$7.43^{+1.38}_{-1.17}$	
HARPS	0.79	$-6.66^{+1.20}_{-1.18}$	$2.19^{+0.39}_{-0.34}$	

HD 30177 c, covering a total timescale of about only 5840 days out of the 31.7 yr proposed orbital period; a fact clearly reflected in the poorly constrained orbital parameters for this proposed outer planet. Moreover, all the MCMC chains we launched in searching for a two-planet solution failed to achieve a satisfactory convergence and parameters resolutions, the acceptance rate never rising above 0.4% and producing exceptionally poorly constrained estimates for the outer companion's orbital parameters, such as a period of $11084.29^{+1235.54}_{-1059.33}$ days and a semi-amplitude of $32.71^{+83.55}_{-26.48}$ m s^{-1}.

We interpret the poor parameter constrains in Wittenmyer et al. (2017) and our repeated failure to achieve a satisfactory convergence as evidence that the most recent literature two-planet fit does not constitute a correct interpretation of the available data. An orbital solution featuring the outer planet as a quadratic trend added to the Keplerian signal of the inner planet may be a better fit to the joined dataset, allowing a further refinement of the orbital parameters for HD 30177 b but only lower limits on the outer planet's semi-amplitude, mass and period.

Following the example set by Kipping et al. (2011) we therefore fitted the radial velocity data for a single Keplerian orbit plus a quadratic term, so that the overall RV model is expressed as

$$RV = V_\gamma - K \sin\frac{2\pi(t - t_{peri})}{P} + k_2(t - t_{pivot}) + \frac{1}{2}k_3(t - t_{pivot})^2 \quad (3)$$

being t_{pivot} the mean time stamp and k_2, k_3 respectively the linear and quadratic coefficients. From this model we can infer some estimate on minimum mass and period for the outer planet using the relationships

$$\frac{-k_2 + k_3 t_{pivot}}{k_3} = t_{peri} + \frac{P}{4}; \quad \frac{k_3}{4\pi^2} = \frac{K}{P^2}. \quad (4)$$

Our best-fit curve (see Table 6 and Fig. 6) returns for planet b values for semi-amplitude $125.98^{+1.26}_{-1.27}$ m s^{-1}, minimum mass of $8.622^{+0.125}_{-0.126}$ M_J, period $2527.83^{+4.71}_{-4.69}$ d and eccentricity $0.162^{+0.010}_{-0.010}$; we find quadratic trend coefficients of $k_2 = (-6.7 \pm 0.5) \times 10^{-3}$ m s^{-1} d^{-1} and $k_2 = (1.20 \pm 0.05) \times 10^{-5}$ m s^{-1}d^{-1}. Again following Kipping et al. (2011), to determine the lower limits for the outer planet's semi-amplitude, mass, and period we force a circular orbit, selecting as minimum svalue of P the one causing a $\delta\chi^2 = 1$ relative to the quadratic fit, and then using this period value for computing a minimum value of K and then minimum mass. The limits thus obtained for the outer planet are $P \geq 6163.40$ d, $K \geq 16.42$ m s^{-1} and $M \sin i \geq 1.533\ M_J$; further datapoints and a greater observation

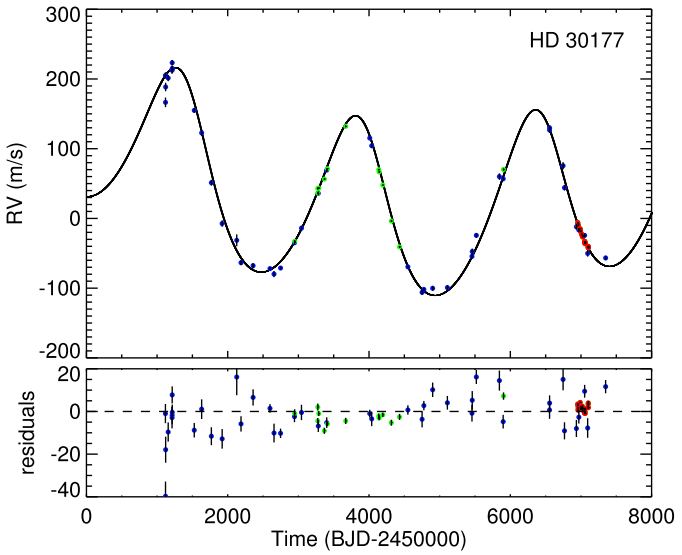

Fig. 6. Same as Fig. 2 but for system HD 30177. The literature AAT data are shown in blue and the literature HARPS data are shown in green; our HARPS survey data are instead shown in red.

Table 7. Fit results comparison for system HD 38801.

HD 38801		
Parameter	Harakawa et al. (2010) Planet b	This work Planet b
K (m s^{-1})	200.0 ± 3.9	$197.29^{+3.52}_{-3.43}$
P (days)	696.3 ± 2.7	$685.25^{+0.85}_{-0.85}$
$\sqrt{e}\cos\omega$	–	$0.089^{+0.058}_{-0.086}$
$\sqrt{e}\sin\omega$	–	$0.021^{+0.087}_{-0.093}$
e	0.0	$0.017^{+0.013}_{-0.011}$
ω (deg)	0.0	$97.115^{+238.614}_{-71.900}$
$M \sin i$ (M_J)	10.7 ± 0.5	$9.698^{+0.573}_{-0.587}$
a (AU)	1.7 ± 0.037	$1.623^{+0.047}_{-0.049}$
T_{peri} (days)	2453966.0 ± 2.1	$2456752.9^{+126.5}_{-102.1}$
n_{obs}	37	58
	Mean RV error (m s^{-1})	γ (m s^{-1})	Jitter (m s^{-1})
Subaru	2.70	$1.44^{+2.96}_{-2.89}$	$10.81^{+2.20}_{-1.71}$
Keck	0.50	$-20.85^{+2.87}_{-2.95}$	$10.93^{+2.76}_{-1.98}$
HARPS	0.45	$175.71^{+4.63}_{-4.77}$	$10.13^{+2.05}_{-1.58}$

Table 8. Fit results comparison for system HD 48265.

HD 48265		
Parameter	Jenkins et al. (2017) Planet b	This work Planet b
K (m s^{-1})	27.7 ± 1.2	$28.65^{+1.59}_{-1.57}$
P (days)	780.3 ± 4.6	$778.51^{+5.38}_{-5.18}$
$\sqrt{e}\cos\omega$	–	$0.298^{+0.104}_{-0.123}$
$\sqrt{e}\sin\omega$	–	$-0.319^{+0.224}_{-0.123}$
e	0.080 ± 0.050	$0.211^{+0.089}_{-0.096}$
ω (deg)	343.78 ± 137.51	$308.313^{+21.261}_{-23.111}$
$M \sin i$ (M_J)	1.47 ± 0.12	$1.525^{+0.049}_{-0.050}$
a (AU)	1.81 ± 0.07	$1.814^{+0.030}_{-0.031}$
T_{peri} (days)	2452892 ± 100	$2456036.7^{+67.7}_{-36.5}$
n_{obs}	60	20
	Mean RV error (m s^{-1})	γ (m s^{-1})	Jitter (m s^{-1})
MIKE	3.22	$-5.81^{+2.29}_{-2.08}$	$3.38^{+1.89}_{-1.53}$
HARPS	0.54	$-6.37^{+2.68}_{-2.72}$	$3.38^{+1.89}_{-1.53}$
CORALIE	9.40	$-1.23^{+4.45}_{-4.49}$	$15.98^{+3.96}_{-3.21}$

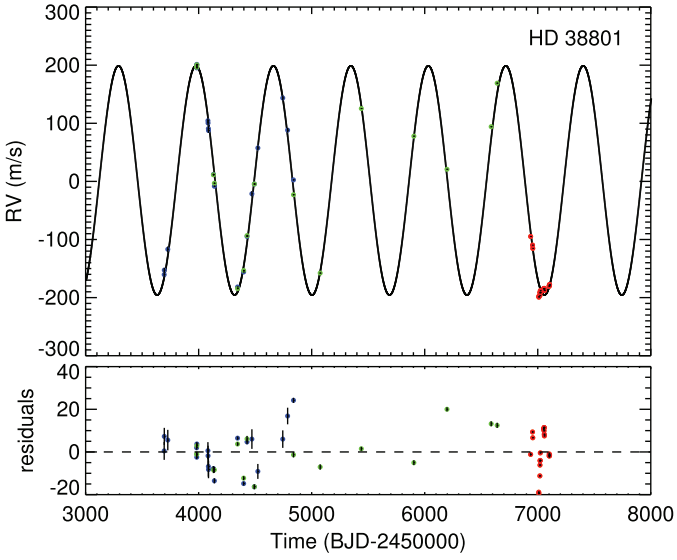

Fig. 7. Same as Fig. 2 but for system HD 38801. The literature Subaru data are shown in blue, literature Keck data is in green, while our HARPS survey data are shown in red.

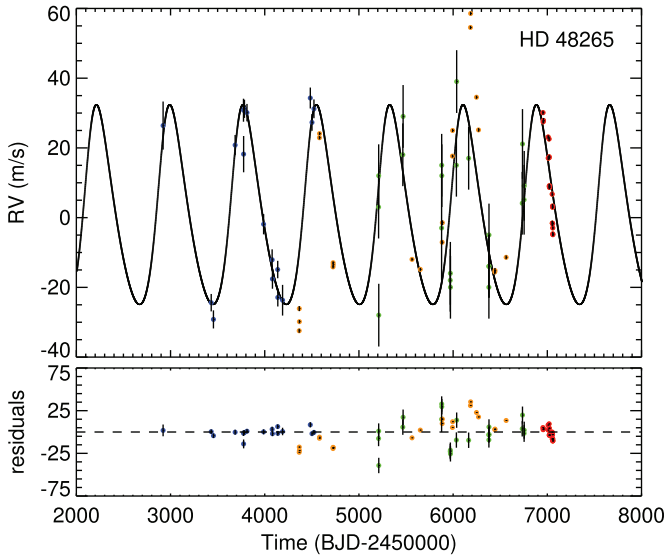

Fig. 8. Same as Fig. 2 but for system HD 48265. The literature MIKE data are shown in blue, the literature HARPS data in orange and literature CORALIE datapoints is in green, while our HARPS survey data are shown in red.

coverage are clearly necessary to better characterize this outer companion.

The most significant peak apparent in the residual data periodogram is located at 771.0 days and has a false alarm probability of 0.1, above our threshold of 1%. The maximum orbital period allowing dynamical stability for an additional inner planet obtained from Hill's criterion is 854.5 days.

HD 38801. This G8IV star is host to a noticeable case of a low-eccentricity super-massive planet discovered by Harakawa et al. (2010), deserving a short literature retrospective. Basing its detection on 21 Subaru and Keck joint observations, the authors reported the results of a Keplerian fit with semi-amplitude 200.0 ± 3.9 m s^{-1} and period of 696.3 ± 2.7 days, obtaining a minimum mass of 10.7 ± 0.5 M_J and an extraordinary low eccentricity, set to zero after its first estimate of 0.04 led to poorly constrained value of ω, also set to zero to improve the fit. HD 38801 b's low eccentricity, the authors note, is of special interest since it cannot be explained by tidal interaction with its host star since the latter's radius of 2.5 $R_\odot$ is too small to effectively circularize the planet's intermediate orbit.

Table 9. Fit results comparison for system HD 50499.

HD 50499			
	Vogt et al. (2005)	This work	
Parameter	Planet b	Planet b	Planet c
K (m s^{-1})	22.9 ± 3	$21.99^{+1.08}_{-1.02}$	≥ 8.15
P (days)	2482.7 ± 110	$2447.10^{+21.92}_{-21.72}$	≥ 8256.51
$\sqrt{e}\cos\omega$	–	$0.161^{+0.084}_{-0.089}$	–
$\sqrt{e}\sin\omega$	–	$-0.483^{+0.046}_{-0.041}$	–
e	0.23 ± 0.14	$0.266^{+0.044}_{-0.044}$	–
ω (deg)	262 ± 36	$288.31^{+9.579}_{-10.094}$	–
$M \sin i$ (M_J)	1.71 ± 0.2	$1.636^{+0.017}_{-0.017}$	≥ 0.942
a (AU)	3.86 ± 0.6	$3.833^{+0.0305}_{-0.030}$	–
T_{peri} (days)	2451234.6 ± 225	$2456291.1^{+58.7}_{-57.6}$	–
n_{obs}	86	24	
	Mean RV error (m s^{-1})	γ (m s^{-1})	Jitter (m s^{-1})
Keck	1.71	$2.33^{+1.05}_{-1.07}$	$5.08^{+0.47}_{-0.42}$
HARPS	0.49	$-18.45^{+3.57}_{-3.55}$	$2.15^{+0.39}_{-0.31}$

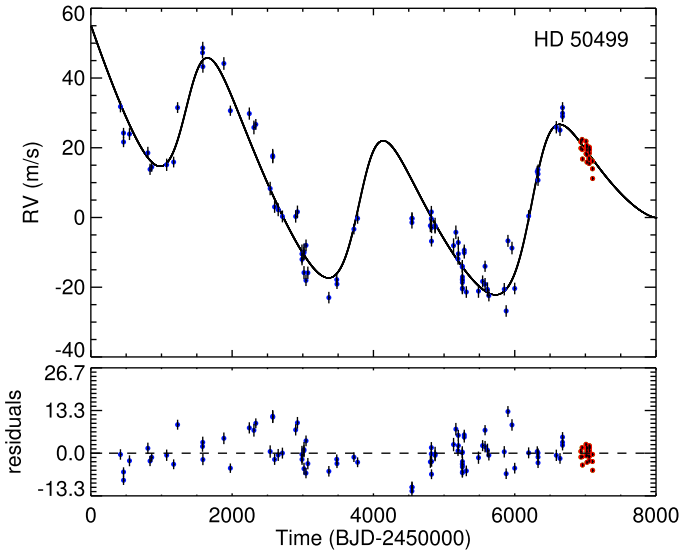

Fig. 9. Same as Fig. 2 but for system HD 50499. The literature Keck data are shown in blue, while our HARPS survey data are shown in red.

The addition of 16 Keck measurments published in Butler et al. (2017) and of our own 21 HARPS measurements allow us to produce a new best-fit solution (see Table 7 and Fig. 7) with semi-amplitude $197.29^{+3.52}_{-3.43}$ m s^{-1} and period $685.25^{+0.85}_{-0.85}$ d, obtaining a minimum mass value of $9.698^{+0.573}_{-0.587}$ M_J and still poorly constrained values for $e = 0.017^{+0.013}_{-0.011}$ and $\omega = 97.115^{+238.614^\circ}_{-71.900}$ that will surely benefit from further high-precision and high-sampling observations. We find the dynamical stability limit period for additional inner planets to be 322.1 days.

A power peak characterized by a very low FAP of 0.01% is present in the residual radial velocity periodogram around 79 days; as shown in Fig. 24 this peak does, however, have a high correlation with similar peaks in the stellar activity indexes, excluding any planetary origin for this signal.

HD 48265. This G5IV star hosts a planet first characterized in Minniti et al. (2009) through the analysis of 17 observations obtained over 4.4 yr with the MIKE echelle spectrograph, and later refined using new HARPS and CORALIE data in Jenkins et al. (2009, 2017).

Our 20 new HARPS observations, when joined with the literature data, lead to a fit characterized by semi-amplitude $K = 28.65^{+1.59}_{-1.57}$ m s^{-1} and period $P = 778.51^{+5.38}_{-5.18}$ d. From this fit (see Table 8 and Fig. 8) we obtain orbital elements $M \sin i = 1.525^{+0.049}_{-0.050}$ and $e = 0.211^{+0.089}_{-0,096}$. Although most of these fit parameters are reasonably consistent with those found by Jenkins et al. (2017), we note that our estimate of eccentricity is only marginally compatible with the one obtained in the published works. The maximum inner period allowing dynamical stability for additional inner planets is found with Hill's criterion to be 294.7 days.

A power peak with FAP = 0.05% is found at 21 days in the residual radial velocity data periodogram, the only stellar activity-related peak at this period being present in the bisector periodogram (see Fig. 25). We therefore tried to find a two-planet solutions for the system, using this residual period and a zero value for eccentricy for the additional planet's initial setting, but found no satisfactory convergence, suggesting that this residual power should be regarded as having stellar origins.

HD 50499. The existence of a planet orbiting this G2V star was first reported by Vogt et al. (2005) based on 35 HIRES observations; in the discovery paper a linear trend of −4.8 m s^{-1}yr^{-1} was also noted, suggesting the presence of an outer companion estimated to be located beyond 4 AU and having a minimum mass of at least 2 M_J. The nature of this additional companion was not completely determined, and although an outer star or brown dwarf were dismissed due to system stability considerations, the proposed two-planet solution was not significantly superior to a model consisting of one planet and a linear trend.

However, the recent publication by Butler et al. (2017) of 50 new Keck measurements taken over 8 yr for HD 50499 shows this outer trend to be parabolic; Butler's work also provides a new reduction of Vogt's datapoints, forming the complete Keck dataset we joined with the 24 HARPS data collected during our observation to refine the orbital solution for HD 50499 b and provide lower limits on the outer planet's mass and period. Following again the example set by Kipping et al. (2011) we fit the radial velocity data for a single Keplerian orbit plus a quadratic term, obtaining a best-fit curve (see Table 9 and Fig. 9) returning for planet b values for semi-amplitude $21.99^{+1.08}_{-1.02}$ m s^{-1}, minimum mass of $1.636^{+0.017}_{-0.017}$ M_J, period $2447 \times 10^{+21.92}_{-21.72}$ d and eccentricity $0.266^{+0.044}_{-0.044}$, in addition to quadratic coefficients $k_2 = (-5.6 \pm 0.3) \times 10^{-3}$ m s^{-1} d^{-1} and $k_2 = (4.6 \pm 0.4) \times 10^{-5}$ m s^{-1} d^{-1}.

We finally derived lower limits for the outer planet orbital parameters as $P \geq 8256.51$ d, $K \geq 8.15$ m s^{-1} and $M \sin i \geq 0.942$ M_J; we additionally note that Kóspál et al. (2009) detects an excess in the star's emission at 70 μm, suggesting the presence of a debris disk at distances larger than 4–5 AU that can provide further constraints on the outer planet's orbital elements; from the outer planet's orbital limits it is possible estimate its major semiaxis as lying beyond ≃8.6 AU and therefore could be placed outside the debris disk. Finally, using Hill's criterion we find the maximum dynamically stable inner period for any additional inner companion to be 959.5 days. The highest power peak in the

Table 10. Fit results comparison for system HD 66428.

	HD 66428	
	Feng et al. (2015)	This work
Parameter	Planet b	Planet b
K (m s^{-1})	52.6 ± 1.1	$54.03^{+1.46}_{-1.43}$
P (days)	2293.9 ± 6.4	$2263.12^{+6.13}_{-5.94}$
$\sqrt{e}\cos\omega$	–	$-0.696^{+0.010}_{-0.010}$
$\sqrt{e}\sin\omega$	–	$-0.086^{+0.025}_{-0.023}$
e	0.440 ± 0.013	$0.493^{+0.015}_{-0.015}$
ω (deg)	180.4 ± 2.6	$187.03^{+1.926}_{-2.07}$
$M \sin i$ (M_J)	3.194 ± 0.060	$3.204^{+0.043}_{-0.043}$
a (AU)	3.471 ± 0.069	$3.467^{+0.024}_{-0.024}$
T_{peri} (days)	2452278 ± 16	$2456857.2^{+7.3}_{-7.4}$
slope (m s^{-1}yr^{-1})	-3.4 ± 0.2	$-2.58^{+0.12}_{-0.12}$
n_{obs}	55	83

	Mean RV error (m s^{-1})	γ (m s^{-1})	Jitter (m s^{-1})
Keck	1.40	$-15.18^{+0.64}_{-0.64}$	$4.00^{+0.55}_{-0.47}$
HARPS	0.68	$18.83^{+1.10}_{-1.01}$	$2.21^{+0.45}_{-0.39}$

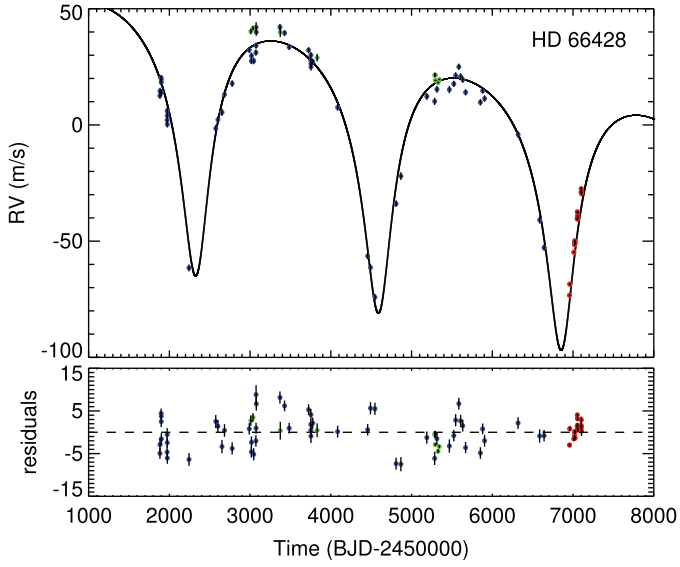

Fig. 10. Same as Fig. 2 but for system HD 66428. The literature Keck data are shown in blue and the literature HARPS observations are shown in green, while our HARPS survey data are shown in red.

Table 11. Fit results comparison for system HD 70642.

	HD 70642	
	Butler et al. (2006)	This work
Parameter	Planet b	Planet b
K (m s^{-1})	30.4 ± 1.3	$30.40^{+1.83}_{-1.91}$
P (days)	2068 ± 39	$2124.54^{+14.65}_{-13.51}$
$\sqrt{e}\cos\omega$	–	$0.020^{+0.108}_{-0.102}$
$\sqrt{e}\sin\omega$	–	$-0.405^{+0.059}_{-0.054}$
e	0.034 ± 0.043	$0.175^{+0.044}_{-0.044}$
ω (deg)	205	$272.840^{+15.584}_{-14.002}$
$M \sin i$ (M_J)	1.97 ± 0.18	$1.993^{+0.018}_{-0.018}$
a (AU)	3.23 ± 0.19	$3.318^{+0.022}_{-0.021}$
T_{peri} (days)	2451350 ± 380	$2456159.1^{+1912.3}_{-131.9}$
n_{obs}	21	50

	Mean RV error (m s^{-1})	γ (m s^{-1})	Jitter (m s^{-1})
AAT	0.75	$-6.71^{+1.22}_{-1.25}$	$3.99^{+1.46}_{-1.26}$
HARPS	0.38	$5.00^{+2.08}_{-2.25}$	$2.24^{+0.38}_{-0.31}$

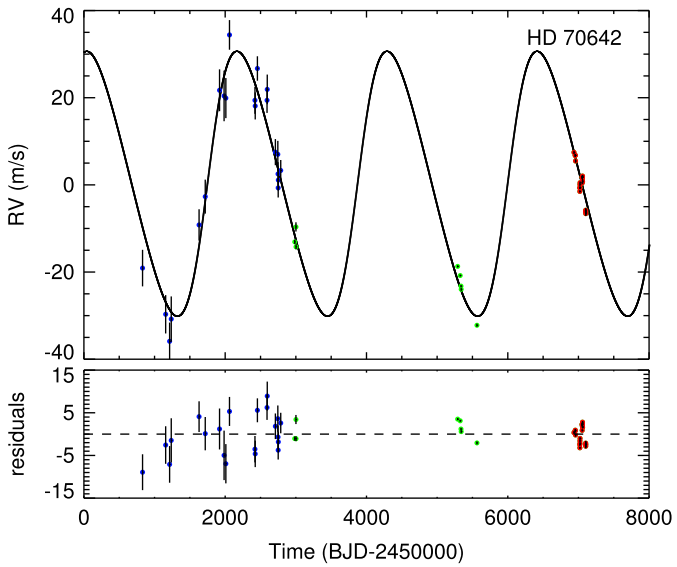

Fig. 11. Same as Fig. 2 but for system HD 70642. The literature AAT data are shown in blue, the literature HARPS data are shown in green while our HARPS survey data are shown in red.

residual periodogram's is found at about 13 days and has a FAP level of 4%, which is above our threshold of 1%.

HD 66428. This G8IV star was first discovered to host a planet in Butler et al. (2006) using 22 Keck observations and its orbital elements were later refined in Feng et al. (2015) using 33 datapoints obtained after the upgrade of HIRES, also reporting a linear trend of -3.4 ± 0.2 m s^{-1}yr^{-1} suggesting the presence of an outer companion.

Combining the improved data reduction published in Butler et al. (2017), 10 HARPS measurements from two different observation periods publicly available on the ESO archive and our own 18 HARPS datapoints we found a best-fit solution for HD 66428 b (see Table 10 and Fig. 10) with $M \sin i = 3.204^{+0.043}_{-0.044}$ M_J, $P = 2263.12^{+6.13}_{-5.94}$ d and $e = 0.493^{+0.015}_{-0.015}$, with a linear trend value of $-2.58^{+0.11}_{-0.12}$ m s^{-1}yr^{-1}. Regarding the system's linear trend and the possible presence of further bodies in the system, we note that Moutou et al. (2017) reports that no additional outer companion above 0.1 $M_\odot$ has been found in the 0.05–50 AU range during a VLT/SPHERE high-angular resolution survey, and therefore the yet undetected source of the slope in the data must be a substellar companion. Following the example set by Feng et al. (2015), we can provide an estimate of the minimum mass required of the companion to produce the

Table 12. Fit results comparison for system HD 73267.

HD 73267		
Parameter	Moutou et al. (2009) Planet b	This work Planet b
K (m s^{-1})	64.29 ± 0.48	$64.65^{+0.86}_{-0.87}$
P (days)	1260 ± 7	$1245.36^{+2.81}_{-2.81}$
$\sqrt{e}\cos\omega$	–	$-0.296^{+0.023}_{-0.022}$
$\sqrt{e}\sin\omega$	–	$-0.376^{+0.021}_{-0.020}$
e	0.256 ± 0.009	$0.230^{+0.014}_{-0.014}$
ω (deg)	229.1 ± 1.8	$231.799^{+3.136}_{-3.286}$
$M \sin i$ (M_J)	3.06 ± 0.07	$3.097^{+0.044}_{-0.043}$
a (AU)	2.198 ± 0.025	$2.187^{+0.016}_{-0.016}$
T_{peri} (days)	2451821.7 ± 16	$2456842.7^{+11.4}_{-12.0}$
slope (m s^{-1}yr^{-1})	–	$2.14^{+0.21}_{-0.19}$
n_{obs}	39	63

	Mean RV error (m s^{-1})	γ (m s^{-1})	Jitter (m s^{-1})
HARPS	1.05	$-9.12^{+0.71}_{-0.71}$	$3.70^{+0.43}_{-0.35}$

Table 13. Fit results comparison for system HD 114729.

HD 114729		
Parameter	Butler et al. (2006) Planet b	This work Planet b
K (m s^{-1})	18.8 ± 1.3	$16.91^{+0.53}_{-0.52}$
P (days)	1114 ± 15	$1121.79^{+3.53}_{-3.43}$
$\sqrt{e}\cos\omega$	–	$0.061^{+0.112}_{-0.124}$
$\sqrt{e}\sin\omega$	–	$0.251^{+0.058}_{-0.086}$
e	0.167 ± 0.055	$0.079^{+0.029}_{-0.032}$
ω (deg)	93 ± 30	$77.059^{+27.681}_{-27.685}$
$M \sin i$ (M_J)	0.95 ± 0.10	$0.825^{+0.007}_{-0.007}$
a (AU)	2.11 ± 0.12	$2.067^{+0.010}_{-0.010}$
T_{peri} (days)	2450520 ± 67	$2454947.7^{+82.4}_{-82.8}$
n_{obs}	52	109

	Mean RV error (m s^{-1})	γ (m s^{-1})	Jitter (m s^{-1})
Keck	1.14	$1.46^{+0.64}_{-0.63}$	$3.93^{+0.50}_{-0.44}$
HARPS	0.22	$-6.11^{+0.41}_{-0.42}$	$2.00^{+0.22}_{-0.19}$

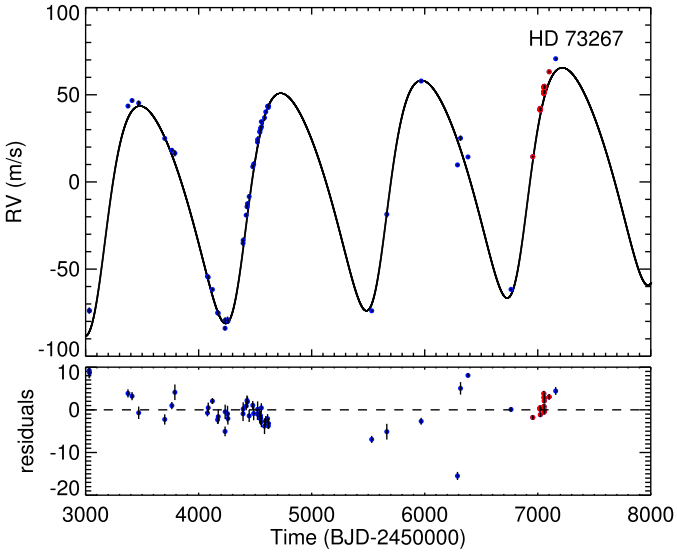

Fig. 12. Same as Fig. 2 but for system HD 73267. The literature HARPS datapoints are shown in blue while our HARPS survey data are shown in red.

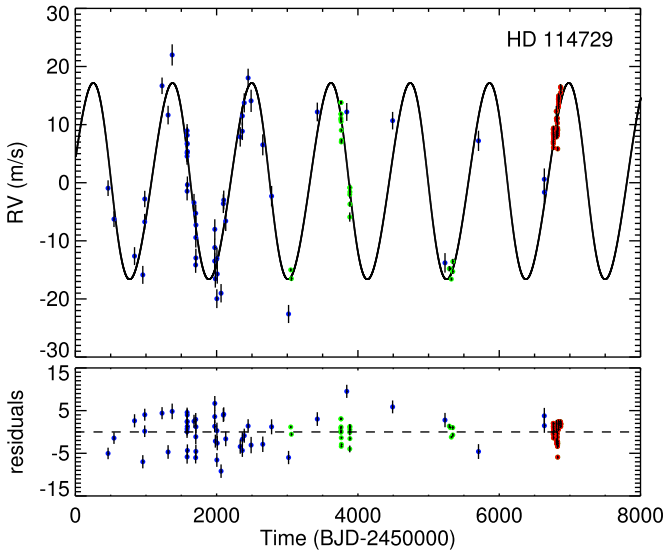

Fig. 13. Same as Fig. 2 but for system HD 114729. The literature Keck data are shown in blue, the literature HARPS data in green, while our HARPS survey data are shown in red.

detected linear slope $\dot{\gamma}$ over the span of observation τ using the equation:

$$M_{min} \approx (0.0164\,M_J)\left(\frac{\tau}{\mathrm{yr}}\right)^{4/3}\left|\frac{\dot{\gamma}}{\mathrm{m\,s^{-1}yr^{-1}}}\right|\left(\frac{M_*}{M_\odot}\right)^{2/3} \quad (5)$$

from which we obtain that the outer companion should have a minimum mass of $1.54\,M_J$, a value not dissimilar from the $1.77\,M_J$ value suggested in the same paper. The maximum period allowing dynamical stability for an additional inner planet is found to be 374.6 days.

No peak with false alarm probability below 0.01 was found in the residual data periodogram.

HD 70642. A G5V star, its known planet was discovered by Carter et al. (2003) using 21 AAT measurements obtained over 5 yr of observations; a more tightly constrained orbital solution was later found in Butler et al. (2006).

In addition to eight archival HARPS datapoints, the acquisition of our 21 high-precision HARPS measurements however lead us to a different orbital solution. We find the best-fit curve (see Table 11 and Fig. 11) to be a Keplerian with semiamplitude $K = 30.40^{+1.83}_{-1.91}$ m s^{-1} and period $P = 2124.54^{+14.65}_{-13.51}$ d; from this we characterize HD 70642 b as having minimum mass $M \sin i = 1.99^{+0.018}_{-0.018}\,M_J$, eccentricity $e = 0.175^{+0.045}_{-0.044}$ and periastron longitude $\omega = 272.840^{+15.584^\circ}_{-14.002}$; the differences in our

Table 14. Fit results comparison for system HD 117207.

HD 117207		
Parameter	Butler et al. (2006) Planet b	This work Planet b
K (m s^{-1})	26.6 ± 0.93	$27.78^{+0.33}_{-0.33}$
P (days)	2597 ± 41	$2621.75^{+8.37}_{-8.53}$
$\sqrt{e}\cos\omega$	–	$-0.001^{+0.038}_{-0.037}$
$\sqrt{e}\sin\omega$	–	$0.394^{+0.016}_{-0.017}$
e	0.144 ± 0.035	$0.157^{+0.013}_{-0.013}$
ω (deg)	73 ± 16	$90.217^{+5.275}_{-5.523}$
$M \sin i$ (M_J)	1.88 ± 0.17	$1.926^{+0.034}_{-0.034}$
a (AU)	3.79 ± 0.22	$3.787^{+0.034}_{-0.035}$
T_{peri} (days)	2450630 ± 120	$2455978.9^{+35.7}_{-37.8}$
n_{obs}	51	140

	Mean RV error (m s^{-1})	γ (m s^{-1})	Jitter (m s^{-1})
Keck	1.54	$-10.58^{+0.52}_{-0.53}$	$3.44^{+0.47}_{-0.40}$
HARPS1	0.35	$4.65^{+0.29}_{-0.29}$	$1.71^{+0.16}_{-0.14}$
HARPS2	0.42	$21.38^{+0.85}_{-0.84}$	$1.88^{+0.55}_{-0.38}$

Table 15. Fit results comparison for system HD 126525.

HD 126525		
Parameter	Mayor et al. (2011) Planet b	This work Planet b
K (m s^{-1})	5.11 ± 0.34	$5.26^{+0.25}_{-0.25}$
P (days)	948.1 ± 22	$960.41^{+6.19}_{-6.33}$
$\sqrt{e}\cos\omega$	–	$0.045^{+0.143}_{-0.151}$
$\sqrt{e}\sin\omega$	–	$-0.071^{+0.151}_{-0.130}$
e	0.13 ± 0.07	$0.035^{+0.039}_{-0.024}$
ω (deg)	–	$247.506^{+76.249}_{-184.079}$
$M \sin i$ (M_J)	0.224 ± 0.0182	$0.237^{+0.002}_{-0.002}$
a (AU)	1.811 ± 0.041	$1.837^{+0.010}_{-0.010}$
T_{peri} (days)	–	$2456161.7^{+534.8}_{-215.7}$
n_{obs}	–	130

	Mean RV error (m s^{-1})	γ (m s^{-1})	Jitter (m s^{-1})
HARPS1	0.45	$-2.18^{+0.18}_{-0.18}$	$1.56^{+0.12}_{-0.10}$
HARPS2	0.41	$16.89^{+0.81}_{-0.80}$	$2.50^{+0.78}_{-0.54}$

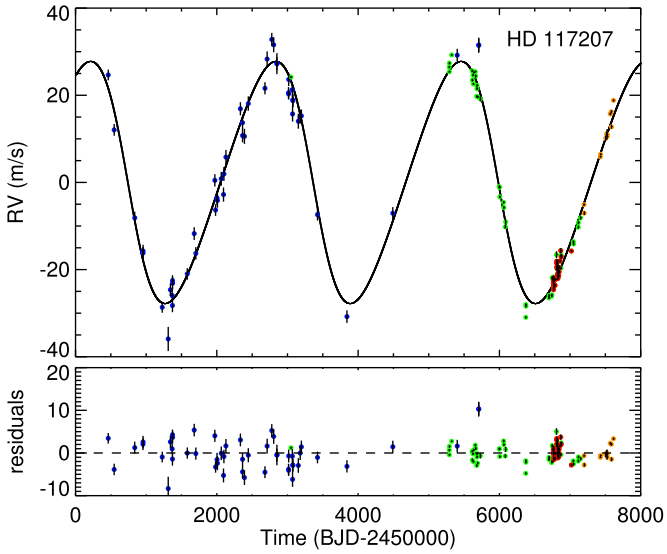

Fig. 14. Same as Fig. 2 but for system HD 117207. The literature Keck data are shown in blue, past HARPS data in green, our HARPS survey data are shown in red while literature HARPS data taken after the fibre-link update of May 2015 are in orange.

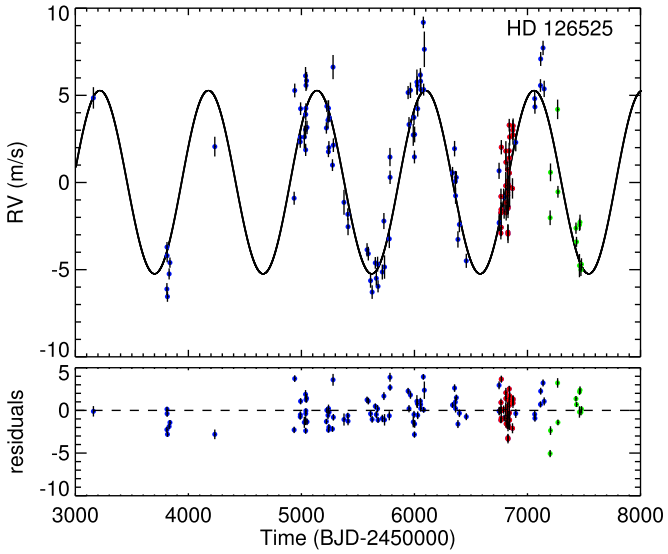

Fig. 15. Same as Fig. 2 but for system HD 126525. Past literature HARPS data are shown in blue, while our HARPS survey data are shown in red and literature HARPS datapoints taken after the fibre-link update of May 2015 are shown in green.

fit are especially evident in the values of P and ω, and we also note that our solution features a poorly constrained value for the time of periastron $T_{peri} = 2456159.1^{+1912.3}_{-131.9}$ d. The maximum period ensuring dynamical stability for an additional inner planet is estimated via Hill's criterion to be 1232.9 days. No residual velocity periodogram peak with a FAP lower than 1% is found.

HD 73267. The planet hosted by this G5V star was discovered using 39 HARPS observations as detailed in Moutou et al. (2009); ten additional archival HARPS data can also be found on the ESO archive. We exclude from the following analysis five literature datapoints taken at epochs 2453781.72, 2454121.74, 2454232.56, 2454257.49, and 2455563.60 for having low S/N.

After joining this literature data with our 17 new HARPS datapoints we found the best-fit curve (see Table 12 and Fig. 12) to have a semi-amplitude value of $64.65^{+0.86}_{-0.87}$ m s^{-1} and period $1245.36^{+2.81}_{-2.81}$ d, from wich values of mass $3.097^{+0.044}_{-0.043}$ M_J and eccentricity $0.230^{+0.014}_{-0.014}$ can be inferred, in good agreement with the literature orbital elements. We also find a previously

Table 16. Fit results comparison for system HD 143361.

HD 143361		
Parameter	Jenkins et al. (2017) Planet b	This work Planet b
K (m s^{-1})	72.1 ± 1	$73.89^{+0.56}_{-0.58}$
P (days)	1046.2 ± 3.2	$1039.15^{+1.64}_{-1.70}$
$\sqrt{e}\cos\omega$	–	$-0.209^{+0.015}_{-0.014}$
$\sqrt{e}\sin\omega$	–	$-0.392^{+0.010}_{-0.009}$
e	0.193 ± 0.015	$0.197^{+0.006}_{-0.006}$
ω (deg)	241.22 ± 3.44	$241.889^{+2.112}_{-2.051}$
$M \sin i$ (M_J)	3.48 ± 0.24	$3.532^{+0.065}_{-0.066}$
a (AU)	1.98 ± 0.07	$1.988^{+0.018}_{-0.018}$
T_{peri} (days)	2453746 ± 147	$2456805.8^{+4.9}_{-4.9}$
n_{obs}	79	107

	Mean RV error (m s^{-1})	γ (m s^{-1})	Jitter (m s^{-1})
MIKE	3.13	$7.50^{+3.87}_{-3.75}$	$11.47^{+3.59}_{-2.49}$
HARPS	0.87	$10.15^{+0.48}_{-0.48}$	$1.86^{+0.25}_{-0.22}$
CORALIE	14.42	$3.31^{+2.09}_{-2.11}$	$2.23^{+2.47}_{-1.57}$

Table 17. Fit results comparison for system HD 152079.

HD 152079		
Parameter	Jenkins et al. (2017) Planet b	This work Planet b
K (m s^{-1})	31.3 ± 1.1	$40.76^{+1.16}_{-1.10}$
P (days)	2899 ± 52	$2918.92^{+37.87}_{-39.28}$
$\sqrt{e}\cos\omega$	–	$0.648^{+0.018}_{-0.018}$
$\sqrt{e}\sin\omega$	–	$-0.331^{+0.025}_{-0.024}$
e	0.52 ± 0.02	$0.532^{+0.015}_{-0.016}$
ω (deg)	324.87 ± 3.44	$332.905^{+2.299}_{-2.195}$
$M \sin i$ (M_J)	2.18 ± 0.17	$2.661^{+0.046}_{-0.046}$
a (AU)	3.98 ± 0.15	$4.187^{+0.051}_{-0.053}$
T_{peri} (days)	2453193 ± 260	$2456173.2^{+11.6}_{-11.3}$
slope (m s^{-1}yr^{-1})	1.72 ± 0.47	$0.35^{+0.24}_{-0.24}$
n_{obs}	46	66

	Mean RV error (m s^{-1})	γ (m s^{-1})	Jitter (m s^{-1})
MIKE	2.98	$-10.34^{+1.51}_{-1.61}$	$4.08^{+1.51}_{-1.22}$
HARPS	0.83	$-7.64^{+0.63}_{-0.63}$	$2.21^{+0.30}_{-0.25}$

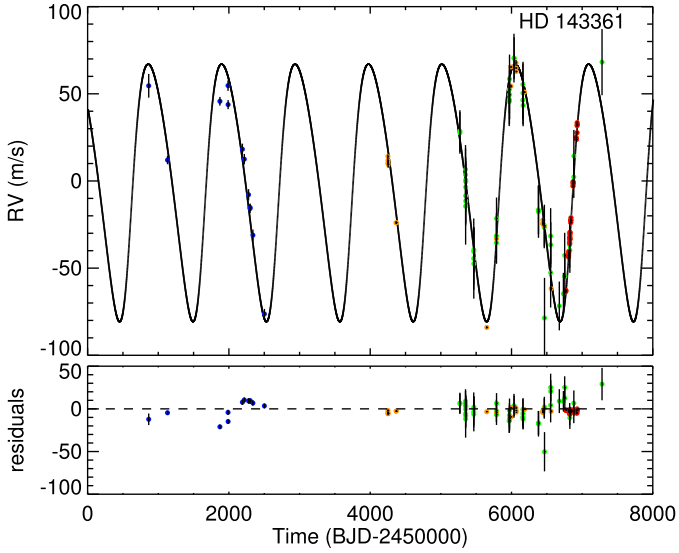

Fig. 16. Same as Fig. 2 but for system HD 143361. The literature MIKE data are shown in blue, literature HARPS data in orange, literature CORALIE datapoints are marked in green, while our HARPS survey data are shown in red.

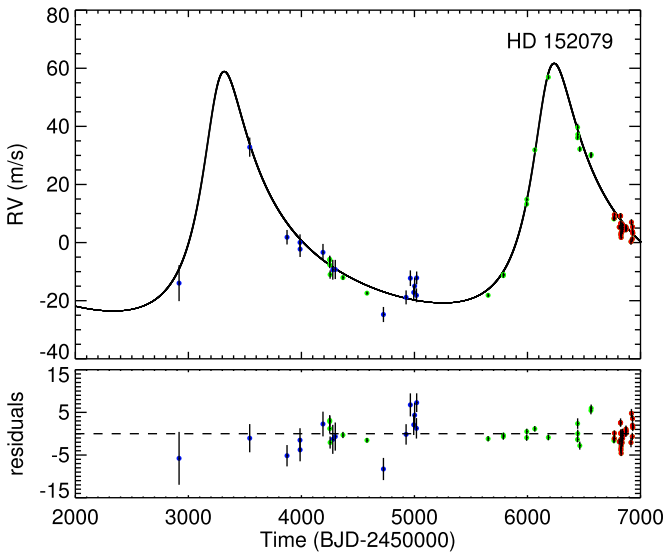

Fig. 17. Same as Fig. 2 but for system HD 152079. Literature MIKE data are shown in blue, literature HARPS data in green while our HARPS survey data are shown in red.

undetected linear trend of $2.14^{+0.20}_{-0.19}$ m s^{-1}yr^{-1}, from which using Eq. (5) we derived a minimum mass of 0.83 M_J for the outer companion. A solution without linear trend was also tested, returning a Bayesian Information Criterion value of 325.25, higher the BIC value of 258.15 returned by the fit featuring a slope, which is therefore preferred. The dynamical stability limit for inner planets is found with Hill's criterion to be 416.5 days. The residual radial velocity periodogram features no peak with a false alarm probability low enough to justify a MCMC search for additional planetary bodies.

HD 114729. The orbital elements of this G0V star's planetary companion were first announced and then refined by Butler et al. (2003, 2006), both results being obtained using Keck data.

Using both the 34 HARPS data collected during our observations and the improvement in Keck data reduction provided in Butler et al. (2017) in addition to 23 archival HARPS datapoint from the ESO Archive we obtained a similar yet better constrained orbital fit (see Table 13 and Fig. 13), producing semi-amplitude $16.91^{+0.53}_{-0.52}$ m s^{-1}, period of $1121.79^{+3.53}_{-3.43}$ days, minimum mass $0.825^{+0.007}_{-0.007}$ M_J and a lower

Table 18. Fit results comparison for system HD 187085.

HD 187085		
Parameter	Jones et al. (2006) Planet b	This work Planet b
K (m s^{-1})	17	$15.39^{+2.21}_{-1.98}$
P (days)	986	$1019.74^{+21.29}_{-22.58}$
$\sqrt{e}\cos\omega$	–	$-0.045^{+0.165}_{-0.186}$
$\sqrt{e}\sin\omega$	–	$0.456^{+0.222}_{-0.448}$
e	0.47	$0.251^{+0.221}_{-0.191}$
ω (deg)	94	$98.315^{+78.336}_{-20.027}$
$M\sin i$ (M_J)	0.75	$0.836^{+0.011}_{-0.011}$
a (AU)	2.05	$2.100^{+0.032}_{-0.032}$
T_{peri} (days)	2450912	$2456053.6^{+252.4}_{-54.4}$
n_{obs}	40	69

	Mean RV error (m s^{-1})	γ (m s^{-1})	Jitter (m s^{-1})
AAT	4.51	$-1.66^{+1.20}_{-1.24}$	$5.51^{+1.15}_{-1.00}$
HARPS	0.59	$-13.50^{+2.06}_{-2.00}$	$1.82^{+0.33}_{-0.27}$

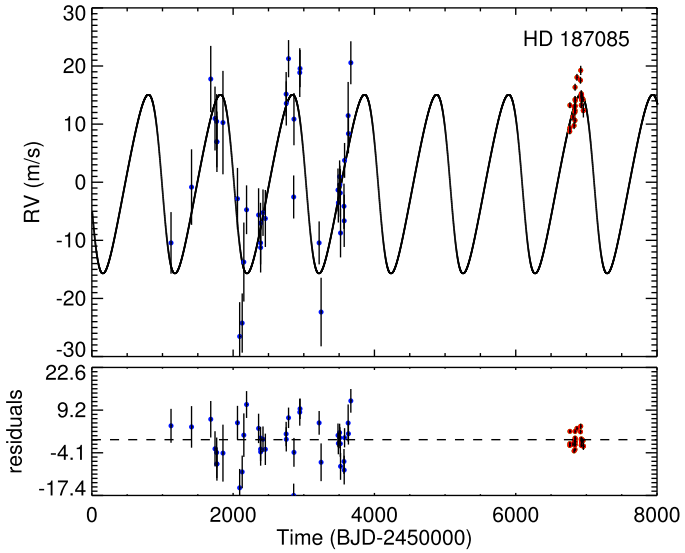

Fig. 18. Same as Fig. 2 but for system HD 187085. The literature AAT data are shown in blue, while our HARPS survey data are shown in red.

eccentricity of $0.0797^{+0.029}_{-0.032}$. Hill's criterion gives us a maximum period of 697.5 days for dynamical stability of inner planets. A major residual periodogram peak at 25 days has a low FAP level of 0.4%; this periodogram peak is however matched by peaks at a similar period in the FWHM and Ca II periodograms (see Fig. 26), suggesting a stellar origin for this power peak.

HD 117207. A G8IV star, its planet was first announced in Marcy et al. (2005) and the orbital solution was later refined by Butler et al. (2006). This literature data were later refined and newly reduced in Butler et al. (2017).

We study the timeseries resulting in joining this newly reduced Keck data, 44 archival HARPS measurements, our own 33 HARPS datapoints and 12 further archival HARPS measurements taken after the May 2015 fibre-link update and that are here therefore treated as a independent dataset. We obtain a a significantly better constrained orbital solution (see Table 14 and Fig. 14), with minimum mass $1.926^{+0.034}_{-0.034}\,M_J$, period of $2621.75^{+8.37}_{-8.53}$ d, eccentricity $0.157^{+0.013}_{-0.013}$ as well as periastron longitude of $90.217^{+5.275^\circ}_{-5.523}$. The maximum period allowing dynamical stability for an inner planet is found with Hill's criterion to be 1263.5 days. No power peak with FAP ≤ 0.01 is found in the residual data periodogram.

HD 126525. This G4V star has been target to various HARPS observational surveys, and Mayor et al. (2011) summary work reports a best-fit solution for its planet; no value for time of periastron passage or longitude is given in the discovery paper, nor the number of measurements used to obtain the orbital solution.

We collected 35 HARPS measurements in our observations, from which we removed a single datapoint at epoch 2456869.5 due to a low S/N value. A total of 96 archival HARPS datapoints were also collected, 11 of which were taken after the fibre-link update of May 2015 and are here treated as an independent dataset.

Joining the literature and the new data we find a fit (see Table 15 and Fig. 15) in which the planet has a minimum mass of $0.237^{+0.002}_{-0.002}\,M_J$, a period of $960.41^{+6.19}_{-6.33}$ d and an eccentricity value of $0.035^{+0.039}_{-0.024}$, a solution generally better constrained than the literature one. The limit on dynamical stability for an additional inner companion is estimated with Hill's criterion to be 707.7 days. No significant peak is found in the residual data periodogram.

HD 143361. The planet orbiting this G6V star was first discovered and reported in Minniti et al. (2009) as the result of 12 MIKE observation, and later studies (Jenkins et al. 2009, 2017) refined the known orbit based on additional HARPS and CORALIE datapoints.

To this literature data, excluding from the 22 HARPS datapoints the three low-S/N measurements taken at epochs 2454253.77, 2454578.78 and 2454581.80, we added our 32 HARPS measurements, from which we exclude a single point at epoch 2456869.62 due to low S/N value. Thus we obtain a best-fit curve (see Table 16 and Fig. 16) of semi-amplitude $73.89^{+0.56}_{-0.58}$ m s^{-1} and a $1039.15^{+1.64}_{-1.70}$ days period, slightly shorter than the literature result. We then obtain a minimum mass of $3.532^{+0.065}_{-0.066}\,M_J$ and an eccentricity value of $0.197^{+0.006}_{-0.006}$, a solution that agrees well with the results of Jenkins et al. (2017) and yet is far better constrained. The residual data periodogram features no major peak with FAP ≤ 0.01.

HD 152079. This G6V star hosts a planet first reported in Arriagada et al. (2010), a discovery based on 15 MIKE datapoints, whose orbit was later refined by Jenkins et al. (2017) using an additional 15 CORALIE measurements and 16 HARPS data in good agreement with Arriagada's first findings, also reporting a linear trend of 1.72 ± 0.47 m s^{-1}yr^{-1}.

We joined our 32 datapoints to the literature timeseries (from which two low-S/N datapoints at epochs 2455649.80 and 2455650.75 were excluded) and additional seven HARPS archival dataponts, obtaining a best-fit (see Table 17 and Fig. 17) solution having $M\sin i = 2.661^{+0.046}_{-0.046}\,M_J$, period of $2918.92^{+37.87}_{-39.28}$ days and eccentricity value of $0.532^{+0.015}_{-0.016}$, also featuring a linear trend of $0.35^{+0.24}_{-0.24}$ m s^{-1} yr^{-1} which, using again Eq. (5), suggests the presence of an outer companion of at least 0.15 M_J. While generally agreeing to the previously published fit, we note that our solution features slightly higher values for planetary mass and major semiaxis and a significantly lower value of linear

Table 19. Fit results comparison for system HD 190647.

HD 190647			
Parameter	Naef et al. (2007) Planet b	This work (short period solution) Planet b	This work (long period solution) Planet b
K (m s^{-1})	36.4 ± 1.2	$32.28^{+0.68}_{-0.66}$	$37.51^{+0.82}_{-0.86}$
P (days)	1038.1 ± 4.9	$878.86^{+1.76}_{-1.65}$	$1176.45^{+3.10}_{-2.83}$
$\sqrt{e}\cos\omega$	–	$-0.071^{+0.042}_{-0.041}$	$-0.364^{+0.038}_{-0.033}$
$\sqrt{e}\sin\omega$	–	$-0.373^{+0.029}_{-0.026}$	$-0.300^{+0.044}_{-0.043}$
e	0.18 ± 0.02	$0.146^{+0.018}_{-0.018}$	$0.224^{+0.014}_{-0.014}$
ω (deg)	232.5 ± 9.4	$259.217^{+6.475}_{-6.744}$	$219.541^{+6.821}_{-6.591}$
$M \sin i$ (M_J)	1.90 ± 0.06	$1.573^{+0.026}_{-0.026}$	$1.985^{+0.033}_{-0.033}$
a (AU)	2.07 ± 0.06	$1.836^{+0.015}_{-0.016}$	$2.231^{+0.019}_{-0.019}$
T_{peri} (days)	2453869 ± 24	$2456552.8^{+16.9}_{-21.0}$	$2457373.0^{+25.2}_{-24.5}$
n_{obs}	20	44	
	Mean RV error (m s^{-1})	γ (m s^{-1}) Jitter (m s^{-1})	γ (m s^{-1}) Jitter (m s^{-1})
HARPS	0.65	$-11.78^{+0.37}_{-0.36}$ $1.32^{+0.22}_{-0.18}$	$-2.62^{+0.61}_{-0.57}$ $1.39^{+0.21}_{-0.17}$
BIC		99.79	101.21

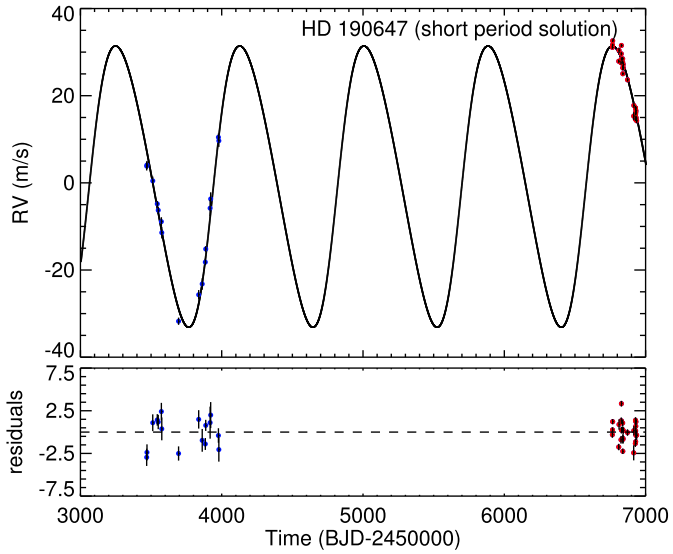

Fig. 19. Same as Fig. 2 but for the short-period solution of system HD 190647. The literature HARPS data are shown in blue, while our HARPS survey data are shown in red.

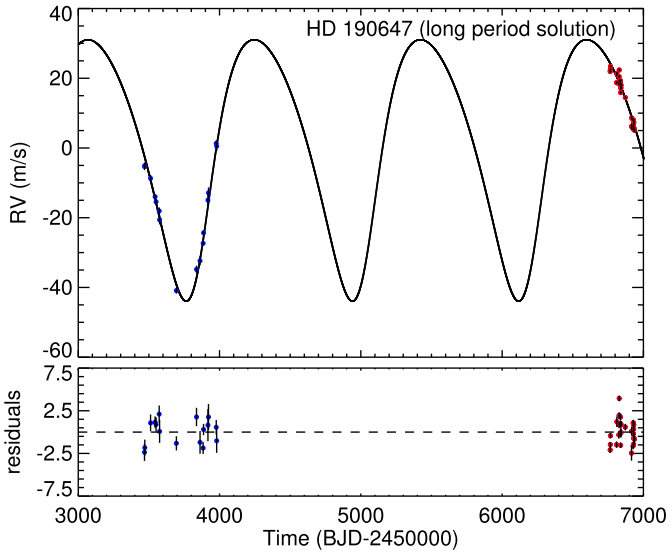

Fig. 20. Same as Fig. 2 but for the long-period solution of system HD 190647. The literature HARPS data are shown in blue, while our HARPS survey data are shown in red.

acceleration. Hill's criterion gives an estimate of 395.9 days for an inner planet's maximum period allowing dynamical stability.

The residual data periodogram features a major peak at 16 days with a false alarm probability of 0.4%. However, significant peaks at similar periods can be found in the periodograms obtained for the activity indexes (see Fig. 27), suggesting a non-planetary origin for the signal.

HD 187085. A G0V star hosting a planet first reported in Jones et al. (2006) using 40 AAT measurements. We note, however, that in the discovery paper the data does not manage to effectively sample the sharp drop evident in the radial velocities, allowing therefore for a better fit characterized by a lower eccentricity.

Our 30 HARPS measurements also fail to sample this sharp drop, therefore not conclusively determining whether a lower value of eccentricity would better fit the data. We also report that the datapoint at epoch 2456825.878, was taken with an erroneous exposure time of five seconds and is therefore ignored in our analysis; the same night (epoch 2456825.884) a new measurement was immediately taken with a correct exposure time of 600 seconds, this one being used instead in our analysis.

We find a new orbital solution (see Table 18 and Fig. 18) with semiaplitude $K = 15.39^{+2.21}_{-1.98}$ m s^{-1}, a longer period of $1019.74^{+21.29}_{-22.58}$ days, slightly higher minimum mass of

Table 20. Fit results comparison for system HD 216437.

HD 216437		
Parameter	Mayor et al. (2004) Planet b	This work Planet b
K (m s^{-1})	34.6 ± 5.7	$39.08^{+1.07}_{-1.04}$
P (days)	1256 ± 35	$1334.28^{+13.07}_{-13.36}$
$\sqrt{e}\cos\omega$	–	$0.237^{+0.051}_{-0.052}$
$\sqrt{e}\sin\omega$	–	$0.509^{+0.026}_{-0.028}$
e	0.29 ± 0.12	$0.317^{+0.028}_{-0.027}$
ω (deg)	63 ± 22	$65.092^{+5.515}_{-5.394}$
$M \sin i$ (M_J)	1.82	$2.223^{+0.058}_{-0.058}$
a (AU)	2.32	$2.497^{+0.036}_{-0.037}$
T_{peri} (days)	2450693 ± 130	$2457289.2^{+52.2}_{-46.6}$
n_{obs}	21	93

	Mean RV error (m s^{-1})	γ (m s^{-1})	Jitter (m s^{-1})
UCLES	3.86	$-0.05^{+1.01}_{-1.02}$	$4.11^{+0.912}_{-0.75}$
CORALIE	5.33	$16.13^{+1.90}_{-1.94}$	$6.47^{+1.96}_{-1.65}$
HARPS	0.32	$-12.41^{+5.06}_{-5.36}$	$2.07^{+0.30}_{-0.25}$

Table 21. Fit results comparison for system HD 220689.

HD 220689		
Parameter	Marmier et al. (2013) Planet b	This work Planet b
K (m s^{-1})	16.4 ± 1.5	$17.12^{+1.26}_{-1.19}$
P (days)	2209^{+103}_{-81}	$2266.40^{+65.84}_{-58.77}$
$\sqrt{e}\cos\omega$	–	$0.090^{+0.161}_{-0.185}$
$\sqrt{e}\sin\omega$	–	$0.059^{+0.176}_{-0.193}$
e	$0.16^{+0.10}_{-0.07}$	$0.054^{+0.061}_{-0.038}$
ω (deg)	137 ± 75	$112.834^{+194.3244}_{-80.118}$
$M \sin i$ (M_J)	1.06 ± 0.09	$1.118^{+0.035}_{-0.035}$
a (AU)	3.36 ± 0.09	$3.396^{+0.084}_{-0.081}$
T_{peri} (days)	245649 ± 413	$2457532.9^{+772.5}_{-478.1}$
n_{obs}	48	79

	Mean RV error (m s^{-1})	γ (m s^{-1})	Jitter (m s^{-1})
CORALIE1	5.67	$6.87^{+2.40}_{-2.51}$	$4.85^{+2.46}_{-2.25}$
CORALIE2	3.48	$-0.07^{+1.38}_{-1.39}$	$6.02^{+1.16}_{-0.95}$
HARPS	0.59	$-9.89^{+3.16}_{-2.66}$	$1.35^{+0.23}_{-0.19}$

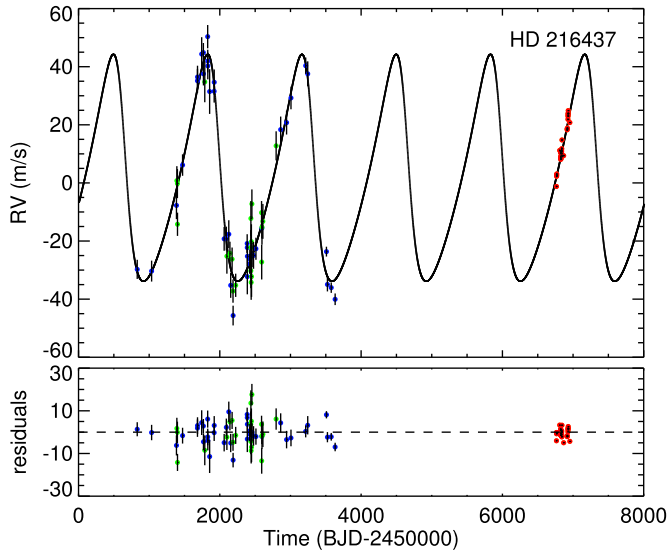

Fig. 21. Same as Fig. 2 but for system HD 216437. The literature UCLES data are shown in blue, CORALIE datapoints are in green while our HARPS survey data are shown in red.

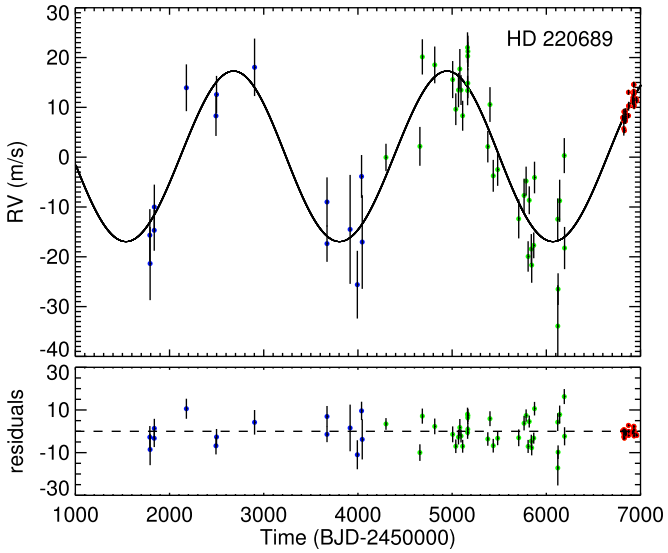

Fig. 22. Same as Fig. 2 but for system HD 220689. The literature CORALIE surveys data are shown in blue and green, while our HARPS survey data are shown in red.

$0.836^{+0.011}_{-0.011}$ M_J and lower but still poorly constrained eccentricity $e = 0.251^{+0.221}_{-0.191}$. Although no uncertainty on the published orbital elements were available in the discovery paper, we note that our solution is generally compatible with the nominal values provided in Jones et al. (2006). We find the highest orbital period allowing stability for an additional inner planet's orbit to be 453.2 days. The residual periodogram show no low FAP significant peak.

HD 190647. This G5V star has been the target of 20 HARPS observations that, as detailed in Naef et al. (2007), led to the discovery of planetary companion HD 190647 b. The authors note however that their data failed to cover the entire orbital period. In the following analysis, we excluded from this literature timeseries the 4 datapoints taken at epochs 2453273.59, 2453274.60, 2453466.90, and 2453493.92 due to low values of S/N.

The 30 HARPS data collected in our survey however manage to sample more efficiently the maximum in RV variation; we removed the datapoint at epoch 2456827.918 since it was taken with an erroneus exposure time of five seconds and another datapoint at epoch 2456840.81 for having low S/N. The resulting timeseries lead to two significantly different possible orbital solutions with similar statistical weight (see Table 19);

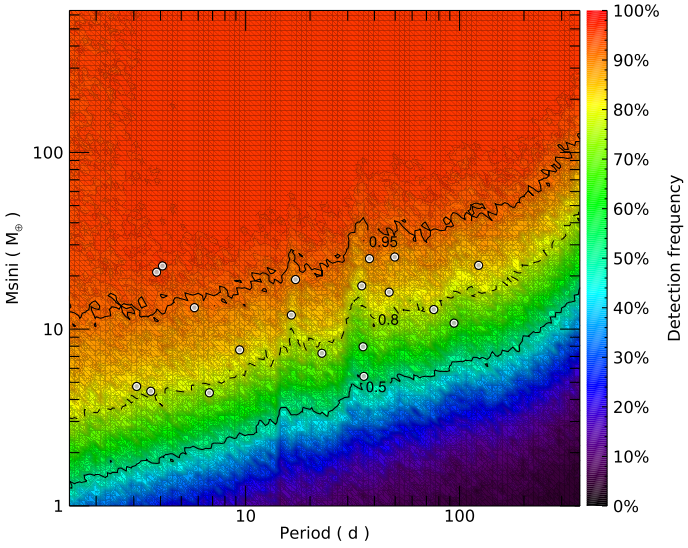

Fig. 23. Colour-coded HARPS precision detection frequency map for the whole 20-systems sample studied in this paper, period ranging from one day to 1 yr and masses ranging from 1 $M_\oplus$ to 2 M_J. The detection frequency levels of 50, 80 and 95% are respectively shown as dotted, dashed and solid curves. The low-mass inner planets of the 11 archival solar system analogues discussed in Sect. 1 are shown as white circles.

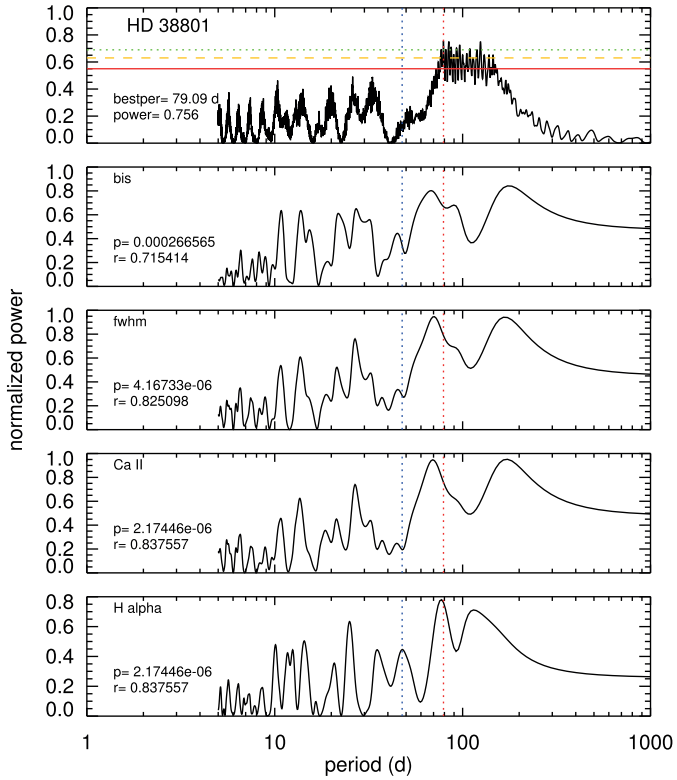

Fig. 24. Activity indexes periodograms for star HD 38801. *Top panel*: post-fit residual data periodogram, the most significant period peak value and power shown in the lower left corner, the horizontal lines indicating the false alarm probability levels of 10% (solid red line), 1% (dashed orange line) and 0.1% (dotted green line). *Following panels*: periodograms for the activity indexes studied in the paper, respectively bisector, FWHM, Ca II and $H\alpha$, the correlation rank r and significance p with the radial velocity residuals shown in each panel's lower left corner. The residual data periodogram's most significant period is highlighted by a vertical red dotted line in all the panels, while the stellar rotation period is shown as a blue dotted vertical line.

since the main difference between these solutions is found in orbital period we shall refer to them as a "short period solution" (see Fig. 19) and a "long period solution" (see Fig. 20). Having respectively a Bayesian Information Criterion value of 99.79 and 101.21 neither solution is clearly preferred.

We characterize the short period solution as having orbital period $878.86^{+1.76}_{-1.65}$ d, radial velocity semi-amplitude $32.28^{+0.68}_{-0.66}$ m s^{-1}, eccentricity of $0.146^{+0.018}_{-0.018}$ and minimum mass of $1.573^{+0.026}_{-0.026}$ M_J. The long period solution features instead a period of $1176.45^{+3.10}_{-2.83}$ d, semi-amplitude $37.51^{+0.82}_{-0.86}$ m s^{-1}, eccentricity of $0.224^{+0.014}_{-0.014}$ and minimum planetary mass $1.985^{+0.033}_{-0.033}$ M_J.

No peak with FAP $\leq$ 0.01 was found in the residual periodogram obtained for either solution. From Hill's criterion we obtain a stability limit maximum period of 527.4 days for an additional inner planet.

HD 216437. A G2IV star whose planetary companion was independently detected by Jones et al. (2002) using 39 UCLES datapoints and by Mayor et al. (2004) with 21 CORALIE observations, finding similar solutions. Using the 33 HARPS datapoint obtained from our observations we find (see Table 20 and Fig. 21) significantly higher values for minimum mass $M \sin i = 2.223^{+0.058}_{-0.058}$ M_J and period $P = 1334.28^{+13.07}_{-13.36}$ d, while the resulting eccentricity value of $e = 0.317^{+0.028}_{-0.027}$ is consistent with the published solution but has a higher accuracy. Hill's criterion gives an orbital period of 427.1 days as a limit on an inner planet's dynamical stability. No low FAP peak is found in the residual data periodogram.

HD 220689. This G3V star's planetary companion discovery was reported in Marmier et al. (2013) after the acquisition of 48 CORALIE datapoints, the last 34 of which were obtained after an instrument upgrade and are therefore treated as an independent dataset. This planet is also notable for having the lowest radial velocity semi-amplitude detected by CORALIE at the time of publication.

Using the 31 HARPS datapoints we collected, we found a compatible but better constrained value for orbital period $P = 2266.40^{+65.84}_{-58.77}$ d, a higher precision value of eccentricity $e = 0.054^{+0.061}_{-0.038}$ and a similarly better determined value of minimum mass $M \sin i = 1.118^{+0.035}_{-0.035}$ M_J (see Table 21 and Fig. 22). We find the maximum period allowing dynamical stability for an additional inner planet to be 1426.6 days. No peak under 1% level of false alarm probability was found in the residual periodogram.

5. Detection limits and planetary frequency

The calculation of the planetary detection frequency in the star sample was carried out using a standard procedure, which is the production of synthetic circular radial velocity curves for different realizations of the orbital elements pair (P, $M \sin i$) and the statistical analysis of the obtained RV curve in order to determine the detection probability of the signal produced by the simulated planet; a recent application of this technique can be seen in Faria et al. (2016).

For each star in our sample we explored 100 different orbital periods P_j evenly spaced in logarithm from a single day to 1 yr and 100 different planetary mass M_k similarly spaced from 1 $M_\oplus$ to 2 M_J. For each one of these period-mass realization we then computed 20 synthetic radial velocity curves, each one with a different randomly obtained combination of ($T_{\rm peri}$, ω); these synthetic radial velocities were obtained by evaluating at each of our survey's observation times t_i the theoretical radial velocity value

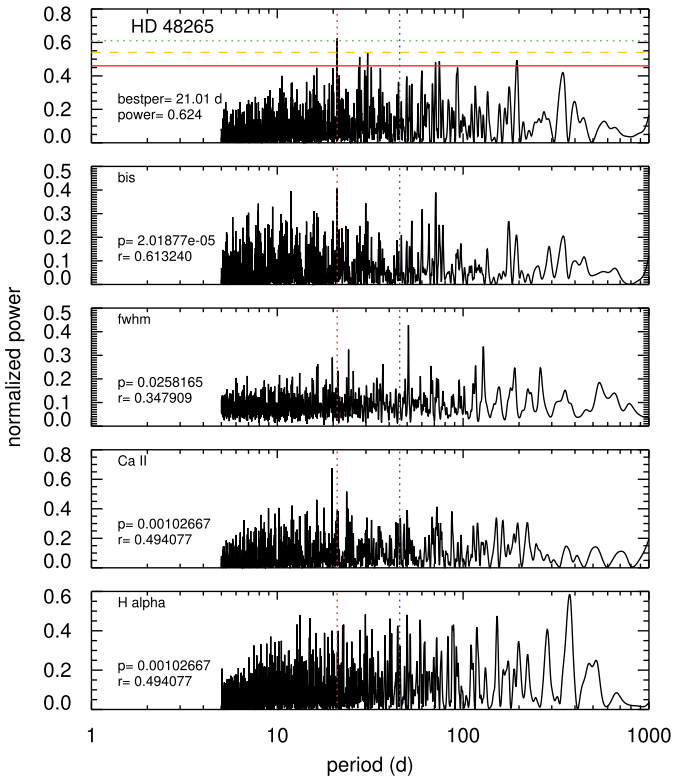

Fig. 25. Same as Fig. 24 but for star HD 48265.

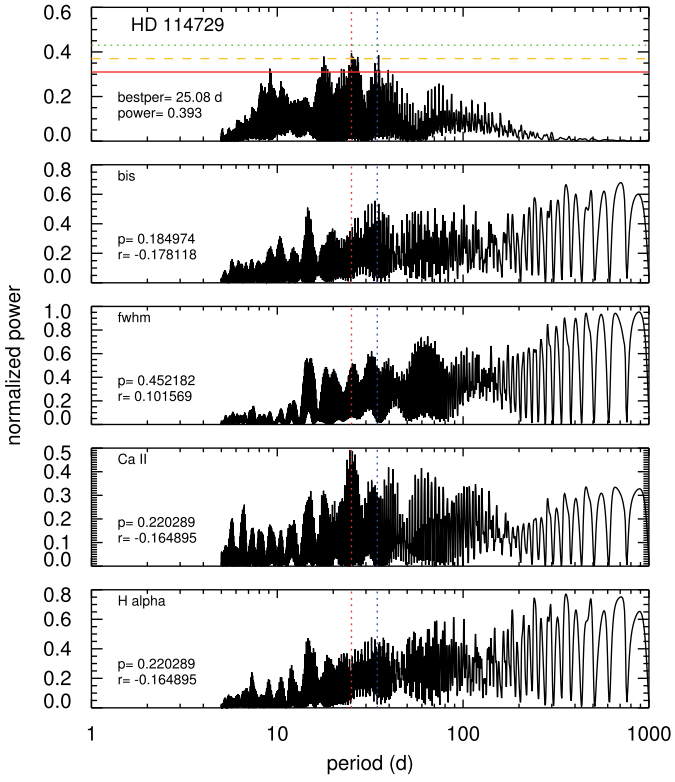

Fig. 26. Same as Fig. 24 but for star HD 114729.

RV($t_i, P_j, M_k, T_{\rm peri}, \omega$) for the injected period and mass, and then adding to this theoretical values a random Gaussian noise with an amplitude equal to the standard deviation of the post-fit residuals data for our high cadence and precision HARPS survey. We then produce a periodogram for each one of the 2×10^5 synthetic signals thus obtained, and the signal is considered as detected only if the injected period power is higher than the power corresponding to a 1% false alarm probability.

It is important to note that our choice to use only our high precision and cadence HARPS residual data for this synthetic curves production leads to a rather conservative evaluation of the detection frequency, being the typical RMS of our post-fit residual data around 3–4 m s^{-1} rather than the ∼0.5 m s^{-1} RMS of our original HARPS data. Also, choosing not to include the lower-precision literature data could lead to some precision loss at high periods, a fact that has however low influence on our analysis since we chose to study detection for periods up to 1 yr. It is also important to note that only in three of the systems of our sample (HD 23127, HD 38801 and HD 48265) a limited portion of the outer region of the period range being considered in this detection limits analysis is subject to instability as calculated throught the Hill criterion (see Sect. 4 and each system's paragraph in Sect. 4.3).

The detection map produced for the overall HARPS survey, obtained summing and renormalizing each and every system's detection map, is shown in Fig. 23. It can be seen that true uniform completeness for the whole 20-star sample is achieved for periods below 50 days only for $M \sin i > 30\ M_\oplus$, while for periods less than 150 days we have whole sample completeness only for $M \sin i > 50\ M_\oplus$. For the same period limits we are instead uniformely sensitive for half our sample respectively for minimum masses ranging from 5 to 10 Earth masses and from 7 to 15 Earth masses. We also note that that for minimum masses ranging from 10 to 30 $M_\oplus$ we have completeness below ten days, a fact that in combination with the lack of additional hot Neptunes found in our analysis suggests a strong absence of such planets around the selected stars.

It is therefore clear that to achieve higher detection frequencies for terrestrial and super-terrestrial planet at all periods, expecially shorter ones, it is necessary to obtain a higher number of observations per target star and ensure a higher-density sampling. Our observing programme, as noted in Sect. 3, originally foresaw about 40 measurements per star, a much higher number than the average 27 per star we actually obtained; it can be argued that a number of observations closer to the one originally proposed could push the survey's detection limits to lower planetary masses, ensuring a better coverage and higher detection frequencies for terrestrial and super-terrestrial additional planets. In fact, analytical expressions for close-in low-mass exoplanets detection threshold found in Narayan et al. (2005) show such a dependence on the number of radial velocity measurements. It will also be important in the near future comparing our results with the similarly produced detection map for the parallel HARPS-N survey mentioned in Sect. 1.

From the overall survey detection map one can finally obtain an estimate for the planetary occurence frequency $f_{\rm p}$ in the presence of a giant outer planet; the probability of obtaining m detection out of a sample of size N is given by the binomial distribution:

$$p(m; N, f_{\rm p}) = \frac{N!}{m!(N-m)!}\, f_{\rm p}^m (1 - f_{\rm p})^{N-m}. \quad (6)$$

The choice of distribution is dictated by the small size of our sample (at most $N = 20$) and has been originally justified in Burgasser et al. (2003) and successfully used in Sozzetti et al. (2009) and Faria et al. (2016), to name a few.

During the analysis of our sample, as detailed in Sect. 4, we found a single new candidate planet, namely the gas giant

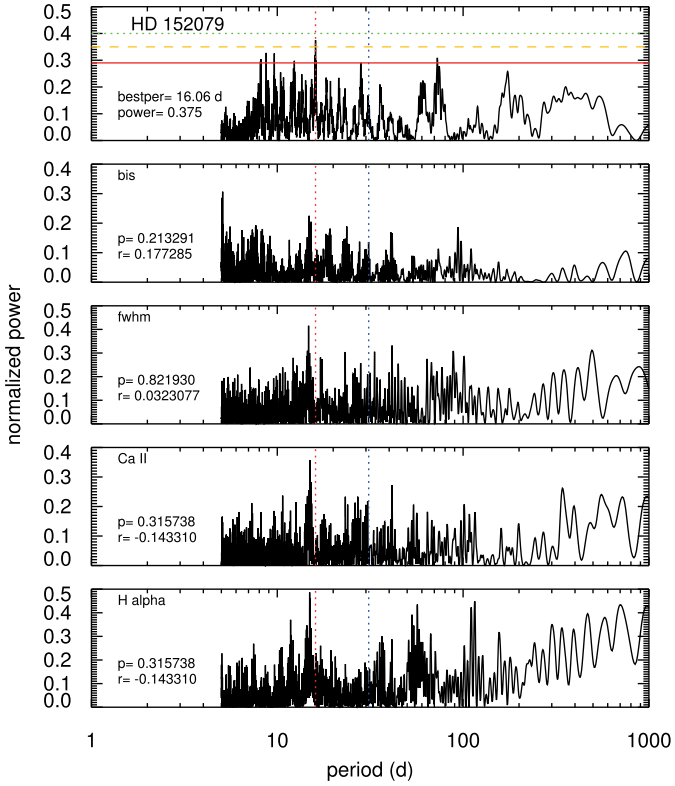

Fig. 27. Same as Fig. 24 but for star HD 152079.

HD 50499 c, which due to its estimated minimum orbital period $P \geq 8265.51$ days lies outside our considered period range of $P \leq 1$ yr. Following a section of the analysis reported in the work of Mayor et al. (2011), in which the authors estimated the occurrence frequency of stars with at leats one planet in given regions of orbital period and planetary mass, we focus our interest on sub-giant planets with orbital period less than 150 days and $M \sin i$ between 10 and 30 $M_{\oplus}$, a region for which we are conservatively sensitive to only 50% of our 20-stars sample. Having found no candidate planet falling within this mass-period space, we can only obtain a lower limit of $1-\sigma$ for the occurence frequency of low-mass planets in the presence of a known outer giant planet of $f_{\rm p} < 9.84\%$, a value we note to be much lower than the $38.8 \pm 7.1\%$ reported in Mayor et al. (2011) for stars hosting at least one planet in the same period-mass region.

6. Summary and discussion

In this work we report the results of an intense observational campaign conducted using the high-precision HARPS spectrograph on 20 stars, obtaining an average of 27 datapoints per star. The stars in the sample were selected in virtue of being bright, inactive and not significantly evolved Sun-like stars hosting at the time of selection a single long-period giant planet previously discovered via radial velocity observations, the final objective of our observations being the search for additional inner low-mass planets and estimating the occurrence frequency of scaled-down solar system analogues.

By combining the literature radial velocity data with our own measurements we have obtained revised orbital solutions for each known planet in our sample using an MCMC-based fitting algorithm, generally characterized by a higher precision on most of the orbital parameters and significant updates on the orbital parameters for half of the selected systems. We especially stress the achievement of a drastically different set of orbital elements for the previously characterized planet HD 30177 c and the characterization of previously unpublished outer giant planet HD 50499 c, both results obtained fitting the data with a Keplerian curve with a parabolic trend. Three of the systems in our sample (HD 66428, HD 73267, and HD 152079) also show a significant slope in the data, one of which (HD 73267) was previously unpublished, suggesting the existence of at least one additional outer companion in the system having a minimum mass >0.83 $M_{\rm J}$.

We have also conducted detection simulations on all sample stars in order to calculate the occurrence rate of inner (periods from one day to 1 yr) low mass (10–30 $M_{\oplus}$) planets in the presence of long-period giants. Having found no candidate planet within these period and mass ranges we can only provide an estimate for the upper limit of said frequency, namely $f_{\rm p} < 9.84\%$, a value which is significantly lower than the one obtained for the same period-mass ranges by Mayor et al. (2011) for stars hosting at least one planet.

The lack of candidate planets found on inner orbits in the sample systems is especially significant when considering again the detection limits of our sample, shown in Fig. 23, from which is clear that we are sensitive to the vast majority of "hot super-Earths" or "mini-Neptunes", defined as planets up to 20 times more massive than the Earth on orbits shorter than 100 days. This type of planet is found to be present around roughly half of all Sun-like stars (Mayor et al. 2011; Howard et al. 2012; Izidoro et al. 2015; Morbidelli & Raymond 2016), often in a compact low-eccentricity configuration within multiple systems, and is noticeably missing in our own solar system. The search for the reason of the lack of hot super-Earth in the solar system has produced several competing formation models for super-Earths (see Morbidelli & Raymond 2016), roughly distinguishable into in situ formation (Hansen & Murray 2012, 2013; Martin & Livio 2016) and inwards-migration processes (Cossou et al. 2014; Izidoro et al. 2015, 2017). The latter model, proposing that super-Earth embryos form in the outer protoplanetary disk before migrating inwards, is especially interesting in interpreting the lack of inner candidate planets found in our sample because, as detailed in Izidoro et al. (2015), if the innermost super-Earth embryo grows into a giant planet core while migrating inwards the newly produced gas giant can and will significantly alter the dynamical evolution of the planetary system, blocking the outer super-Earths from further inwards-migration, with some embryos only occasionally crossing the giant planet's orbit and becoming hot super-Earths or mini-Neptunes. While some studies (Volk & Gladman 2015; Batygin & Laughlin 2015) propose that the early solar system hosted a close-in population of super-Earths that was either destroyed by erosive collisions or by merging with the Sun, Izidoro & Raymond (2018) points out that the debris generated by erosive processes should have catalyzed further growth of close-in planets and that the existence of an inner edge in the protoplanetary disk should actually prevent planets from simply falling onto the Sun, suggesting instead that the wide, low-eccentricity orbit of Jupiter has had a key role in effectively blocking the formation of close-in super-Earths in the solar system. The lack of planets found on inner orbits in our sample could be interpreted as evidence for the main observational prediction of the inwards-migration model, namely the anti-correlation between planetary systems hosting close-in super-Earths and those hosting long-period gas giants.

There is also an interesting formal match between the occurence rate 9.84% of low mass planets in the presence of outer

giants derived from our analysis and the preliminary ∼10% fraction of solar system analogues discussed in Sect. 1 that we found amongst the multi-planet systems studied via the radial velocity method; it is also interesting to note from Fig. 23 that the inner low-mass planets in these 11 systems would have been detected by our survey in at least 50% of the cases. It could be also argued that the low number of low-mass inner planets in these systems could be examples of the planetary embryos that can occasionally cross the innermost giant planet's orbit in the inwards-migration formation scenario. However, we stress that the 11 multi-planet systems are not a homogeneous sample, showing a variety of stellar type and planetary characteristics and that were selected in our preliminary search in virtue of the relation between planetary orbits in relation and the circumstellar habitable zone, while the 20-stars sample that is the main focus of this work were all homogeneously selected for their stellar characteristics (as detailed in Sect. 2) and that we did not focus on their habitable zone. While it is interesting to note a suppression of this type of planetary architecture across different spectral types, directly comparing such differently selected groups of systems to draw supportable conclusions about their dynamical history is difficult without further data and higher statistics and beyond the scope of this work.

We finally stress the need for further high-cadence and high-precision observations of the sample stars in order to better characterize certain systems; in particular the constrains on some planets eccentricity and longitude of periastron, such as HD 38801 b and HD 126525 b will greatly benefit from additional intense observations. Exceptional attention will surely be needed in future observations of systems HD 30177 and HD 50499, whose long-period (respectively ≃17 and ≃22 yr) outer planet orbits are still incompletely sampled and therefore only partially characterized via semi-amplitude, period and mass lower limits.

As a final and future-orientated point of interest we estimated the astrometric signal α of each known giant planet in our sample, using the relation

$$\alpha = \frac{M_{\rm p}}{M_*}\frac{a}{d} \tag{7}$$

in order to obtain a quick evaluation of how many and which systems in our sample could be observed by the high-precision astrometric satellite *Gaia* during its ongoing 5-yr mission, to fuel further instrument synergies. We find 13 of our systems (namely HD 27631, HD 30177, HD 38801, HD 50499, HD 66428, HD 70642, HD 73267, HD 117207, HD 143361, HD 152079, HD 190647, HD 216437, and HD 220689) to have an astrometric signal $\alpha \gtrsim 50\,\mu$ as (expected to be detected by *Gaia* at high S/N); being however α obviously dependent on the planet's true mass this fraction of astrometrically observable planets could very well be much higher if their orbital inclination turns out to be rather small in value. The importance of evaluating which systems could be observed by *Gaia* is clear when considering that during its 5-yr mission the satellite will provide a partial or complete coverage of the known planet's orbit. It will, therefore, produce a high-accuracy dataset that could be combined with the literature radial velocity data to further constrain the systems orbital elements and search for additional inner companions in the residuals. This is an important example of how using different detection methods and instruments can and will help future detailed analysis on exoplanetary systems architecture Figs. 24–27.

Acknowledgements. We thank the anonymous referee for useful comments. DB acknowledges financial support from INAF and Agenzia Spaziale Italiana (ASI grant n. 014-025-R.1.2015) for the 2016 PhD fellowship programme of INAF. MD acknowledges funding from INAF through the Progetti Premiali funding scheme of the Italian Ministry of Education, University, and Research. The research leading to these results has received funding from the European Union Seventh Framework Programme (FP7/2007-2013) under Grant Agreement No. 313014 (ETAEARTH).

References

Arriagada, P., Butler, R. P., Minniti, D., et al. 2010, ApJ, 711, 1229
Batygin, K., & Laughlin, G. 2015, Proc. Natl. Acad. Sci., 112, 4214
Bonfanti, A., Ortolani, S., Piotto, G., & Nascimbeni, V. 2015, A&A, 575, A18
Burgasser, A. J., Kirkpatrick, J. D., Reid, I. N., et al. 2003, ApJ, 586, 512
Butler, R. P., Marcy, G. W., Vogt, S. S., et al. 2003, ApJ, 582, 455
Butler, R. P., Wright, J. T., Marcy, G. W., et al. 2006, ApJ, 646, 505
Butler, R. P., Vogt, S. S., Laughlin, G., et al. 2017, AJ, 153, 208
Cabrera, J., Csizmadia, S., Lehmann, H., et al. 2014, ApJ, 781, 18
Carter, B. D., Butler, R. P., Tinney, C. G., et al. 2003, ApJ, 593, L43
Ciardi, D. R., Fabrycky, D. C., Ford, E. B., et al. 2013, ApJ, 763, 41
Cossou, C., Raymond, S. N., Hersant, F., & Pierens, A. 2014, A&A, 569, A56
da Silva, L., Girardi, L., Pasquini, L., et al. 2006, A&A, 458, 609
Eastman, J., Gaudi, B. S., & Agol, E. 2013, PASP, 125, 83
Faria, J. P., Santos, N. C., Figueira, P., et al. 2016, A&A, 589, A25
Feng, Y. K., Wright, J. T., Nelson, B., et al. 2015, ApJ, 800, 22
Hansen, B. M. S., & Murray, N. 2012, ApJ, 751, 158
Hansen, B. M. S., & Murray, N. 2013, ApJ, 775, 53
Harakawa, H., Sato, B., Fischer, D. A., et al. 2010, ApJ, 715, 550
Hobson, M. J., & Gomez, M. 2017, New Ast., 55, 1
Howard, A. W., Marcy, G. W., Bryson, S. T., et al. 2012, ApJ, 201, 15
Izidoro, A., & Raymond, S. N. 2018, ArXiv e-prints [arXiv: 1803.08830]
Izidoro, A., Raymond, S. N., Morbidelli, A., Hersant, F., & Pierens, A. 2015, ApJ, 800, L22
Izidoro, A., Ogihara, M., Raymond, S. N., et al. 2017, MNRAS, 470, 1750
Jenkins, J. S., Jones, H. R. A., Goździewski, K., et al. 2009, MNRAS, 398, 911
Jenkins, J. S., Jones, H. R. A., Tuomi, M., et al. 2017, MNRAS, 466, 443
Jones, H. R. A., Paul Butler, R., Marcy, G. W., et al. 2002, MNRAS, 337, 1170
Jones, H. R. A., Butler, R. P., Tinney, C. G., et al. 2006, MNRAS, 369, 249
Kipping, D. M., Hartman, J., Bakos, G. Á., et al. 2011, AJ, 142, 95
Kopparapu, R. K., Ramirez, R., Kasting, J. F., et al. 2013, ApJ, 765, 131
Kóspál, Á., Ardila, D. R., Moór, A., & Ábrahám, P. 2009, ApJ, 700, L73
Mamajek, E. E., & Hillenbrand, L. A. 2008, ApJ, 687, 1264
Marcy, G. W., Butler, R. P., Vogt, S. S., et al. 2005, ApJ, 619, 570
Marmier, M., Ségransan, D., Udry, S., et al. 2013, A&A, 551, A90
Martin, R. G., & Livio, M. 2016, ApJ, 822, 90
Mayor, M., Udry, S., Naef, D., et al. 2004, A&A, 415, 391
Mayor, M., Marmier, M., Lovis, C., et al. 2011, ArXiv e-prints [arXiv: 1109.2497]
Minniti, D., Butler, R. P., López-Morales, M., et al. 2009, ApJ, 693, 1424
Morbidelli, A., & Raymond, S. N. 2016, J. Geophys. Res. (Planets), 121, 1962
Moutou, C., Mayor, M., Lo Curto, G., et al. 2009, A&A, 496, 513
Moutou, C., Mayor, M., Lo Curto, G., et al. 2011, A&A, 527, A63
Moutou, C., Vigan, A., Mesa, D., et al. 2017, A&A, 602, A87
Murray, C. D., & Dermott, S. F. 1999, Solar System Dynamics (Cambridge University Press)
Naef, D., Mayor, M., Benz, W., et al. 2007, A&A, 470, 721
Narayan, R., Cumming, A., & Lin, D. N. C. 2005, ApJ, 620, 1002
Noyes, R. W., Hartmann, L. W., Baliunas, S. L., Duncan, D. K., & Vaughan, A. H. 1984, ApJ, 279, 763
O'Toole, S. J., Butler, R. P., Tinney, C. G., et al. 2007, ApJ, 660, 1636
Raymond, S. N., Barnes, R., & Mandell, A. M. 2008, MNRAS, 384, 663
Sahlmann, J., Lazorenko, P. F., Ségransan, D., et al. 2016, A&A, 595, A77
Schlaufman, K. C. 2014, ApJ, 790, 91
Sousa, S. G., Santos, N. C., Mayor, M., et al. 2008, A&A, 487, 373
Sozzetti, A., Torres, G., Latham, D. W., et al. 2009, ApJ, 697, 544
Stassun, K. G., Collins, K. A., & Gaudi, B. S. 2017, AJ, 153, 136
Tinney, C. G., Butler, R. P., Marcy, G. W., et al. 2003, ApJ, 587, 423
Vogt, S. S., Butler, R. P., Marcy, G. W., et al. 2002, ApJ, 568, 352
Vogt, S. S., Butler, R. P., Marcy, G. W., et al. 2005, ApJ, 632, 638
Volk, K., & Gladman, B. 2015, ApJ, 806, L26
Winn, J. N., & Fabrycky, D. C. 2015, ARA&A, 53, 409
Wittenmyer, R. A., Horner, J., Mengel, M. W., et al. 2017, AJ, 153, 167
Zechmeister, M., & Kürster, M. 2009, A&A, 496, 577